HORIZON 2020

RESEARCH INFRASTRUCTURES

H2020-INFRAIA-2014-2015

INFRAIA-1-2014-2015 INTEGRATING AND OPENING EXISTING NATIONAL AND REGIONAL RESEARCH INFRASTRUCTURES OF EUROPEAN INTEREST

ENSAR2

EUROPEAN NUCLEAR SCIENCE AND APPLICATION RESEARCH 2

GRANT AGREEMENT NUMBER: 654002

DELIVERABLE D5.3 – NUCLEAR PHYSICS INSTRUMENTATION FOR MEDICINE

Version: 3.0
Author: P.G. Thirolf with contributions from MediNet participants
Date: 15.02.2019

PROJECT AND DELIVERABLE INFORMATION SHEET

ENSAR2 Project Ref. №	654002
Project Title	European Nuclear Science and Application Research 2
Project Web Site	http://www.ensarfp7.eu/
Deliverable ID	D5.3
Deliverable Nature	Report
Deliverable Level*	PU
Contractual Date of Delivery	28.02.2019
Actual Date of Delivery	28.02.2019
EC Project Officer	Mina Koleva

* The dissemination level are indicated as follows: PU – Public, PP – Restricted to other participants (including the Commission Services), RE – Restricted to a group specified by the consortium (including the Commission Services). CO – Confidential, only for members of the consortium (including the Commission Services).

DOCUMENT CONTROL SHEET

Document	Title: Nuclear Physics Instrumentation for Medicine	
	ID: D5.3	
	Version 3.0	
	Available at: http://www.ensarfp7.eu/	
	Software Tool: Microsoft Office Word 2007	
	File: ENSAR2_Deliverable_5.3	
Authorship	Written by:	P.G. Thirolf
	Contributors:	NA5 MediNet WP Participants of Task 1
	Reviewed by:	B. Jones
	Approved by:	K. Turzo

DOCUMENT STATUS SHEET

Version	Date	Status	Comments
V0.2	15.12.2018	For internal review	Formal framework, first topical input
V1.0	16.12.2018	For internal review	Added contributions from Munich, Dresden, Valencia, Madrid, Groningen
V1.1	25.12.2018	For internal review	Added contributions from Pisa, Coimbra, Clermont-Ferrand, Lyon, Grenoble
V1.2	01.01.2019	For internal review	Added contribution from U Rome
V2.0	07.01.2019	For internal review	Edited references, executive summary

V2.1	08.01.2019	For internal review	Added concluding remarks
V3.0	21.01.2019	For internal review	After feedback round
V4.0	15.02.2019	After internal review	Revised and submitted

Document Keywords

Keywords	Particle therapy, medical imaging, positron emission tomography, prompt gamma imaging, single-photon emission computed tomography, radiation detectors

Disclaimer

This deliverable has been prepared by Work Package 5 (MediNet – Network: Nuclear Physics for Medicine) of the Project in accordance with the Consortium Agreement and the Grant Agreement n°654002. It solely reflects the opinion of the parties to such agreements on a collective basis in the context of the Project and to the extent foreseen in such agreements.

Copyright notices

TABLE OF CONTENTS

LIST OF FIGURES

LIST OF ACRONYMS AND ABBREVIATIONS

Accuray	Company that provides devices for precise radiotherapy (e.g Cyberknife)
AGOR	superconducting K=600 MeV cyclotron for the acceleration of both light and heavy ions at KVI-CART (The Netherlands)
APD	Avalanche photo diode
ASIC	Application Specific Integrated Circuit
ATCA	Advanced Telecommunications Computing Architecture: Standard for bus-driven electronics, designed for high capacity and high-end applications
BGO	Bismuth germanate (Bi4Ge3O12): scintillation detector crystal material
BNCT	Boron neutron capture therapy
CAL	Centre Antoine Lacassagne: proton therapy center at Nice/France
CCD	Charge coupled device : silicon based photosensor chip with frame-wise readout, commonly used, e.g., for digital photography devices
$CeBr_3$	Cerium bromide: scintillation detector crystal material
CERN	Centre Europeen de Recherche Nucleaire
CLaRyS	Contrôle en Ligne de l'hadrontherapie par Rayonnements Secondaires : French collaboration for online control of hadron therapy via secondary radiation
CNAO	Centro Nazionale di Adroterapia Oncologica (Pavia/Italy)
CNA	Centro Nacional de Acceleradores: National particle accelerator center at Sevilla, Spain
CPP	Centre of Physics of Particles of Marseille
CREATIS	Centre for research into the acquisition and processing of images for healthcare at Univ. Lyon/France
CRT	Coincidence resolving time
CsI	Cesium iodide: scintillation detector crystal material
CT	Computed Tomography is a medical imaging technique using a large series of two-dimensional X-ray images.
CVD	Chemical Vapor Deposition: commercial method to produce synthetic diamonds
Cyberknife	robotic radiosurgery system for tumor treatment with photon beams (manufactured by Accuray)
CZT	Cadmium-Zinc-Telluride: semiconductor detector material
D	Absorbed dose is a measure of the energy deposited per unit mass of medium by ionising radiation, and so has the unit Gy.
DAQ	Data acquisition
DNA	Deoxyribonucleic acid: molecule that carries the genetic instructions used in the growth, development, functioning and reproduction of all known living organisms
DOI	Depth of interaction: source of parallax error in PET image reconstruction
DP	Dose profiler
dSiPM	Digital silicon photomultiplier: semiconductor-based photosensor with built-in digital signal processing components
DPGA	détecteur pixelisé de grande acceptance, i.e. pixelated detector with large acceptance (realized at LPC Clermont-Ferrand/France)
ENSAR2	European Nuclear Science And Applications: EU-funded Integrating Initiative with the 'Horizon 2020' funding framework of the EU
ESRF	European Synchrotron Research Facility (Synchtrotron light source located at Grenable/France)

eV	Practical unit for energy used in atomic and nuclear physics (e.g. for particle beam energy): 1 eV = 1.6x 10^{-19} J
FDG	Fluorodeoxyglucose is a radiopharmaceutical used in PET imaging.
FoV	Field of View: area in the view of an optical or imaging device
FWHM	Full Width at Half Maximum: measure for the width of a spectral line or peak of a distribution
γ-PET	Gamma-PET (also: triple PET or WGI, i.e. whole gamma imaging): variant of the PET imaging modality with 3 photons, where a third prompt photon is emitted from the deexcitation of the β^+ daughter isotope (like ^{10}C).
GAGG	Gadolinium Aluminium Gallium Garnet ($Gd_3Al_2Ga_3O_{12}$), doped with Ce is a newly developed scintillator material
GATE	Geant4 Application for Tomographic Emission: (open source) simulation toolkit dedicated to numerical simulations in medical imaging and radiotherapy (maintained by the international OpenGate collaboration)
GFN	Grupo Fisica Nuclear: nuclear physics group at Madrid/Spain
GHz	1 billion Hertz (oscillations per second)
GEANT4	Geant4 is a toolkit for the simulation of the passage of particles through matter. Its areas of application include high energy, nuclear and accelerator physics, as well as studies in medical and space science.
GSI	Gesellschaft für SchwerIonenforschung – Centre for Heavy Ion Research located at Darmstadt, Germany
Gy	Gray is the name of the special unit of absorbed dose of ionising radiation, i. e. the absorption of one joule of ionising radiation by one kilogram of matter. 1Gy = 1 J/kg = 1 m^2/s^2
HDR	High Dose Rate
HITACHI	Japanese manufacturer of (amongst others) medical accelerator systems
IBA	Ion Beam Applications: Market leading provider of proton therapy facilities and auxiliary systems (headquarter located in Louvain-la-Neuve, Belgium)
ICRU	International Commission on Radiation Units and Measurements is a standardisation body set up in 1925 by the International Congress of Radiology.
ID17	Specific beamline at the European Synchrotron Light Source ESRF in Grenoble/France
IFJ PAN	Instytut Fizyki Jądrowej, Polish Academy of Sciences (Krakow/Poland)
IFIC	Institut de Fisica Corpuscular (Particle Physics Institute): research institution at Valencia/Spain
IMRT	Intensity-Modulated Radiation Therapy is an advanced type of high-precision radiation therapy technique.
INFN	Istituto Nazionale di Fisica Nucleare, Italy
INSIDE	INnovativeSolutIons for Dosimetry in HadronthErapy: is an innovative bimodal imaging system providing a robust method of ion range verification during particle therapy treatments. Developed in a collaboration between the University of Pisa, the University of Rome "Sapienza", the University of Turin, Politecnico of Bari and the National Institute of Nuclear Physics (INFN) and, for the clinical trial, the National Center for Oncological Hadrontherapy (CNAO)
IPNL	Institut de Physique Nucleaire de Lyon (Lyon/France)
IRIS	Image Reconstruction, Instrumentation and Simulations for medical imaging applications: acronym for the corresponding research group at IFIC Valencia

KETEK	Munich-based manufacturer of silicon photomultiplier tubes
k-NN	k nearest neighbor: algorithm for determining the photon interaction position in a monolithic scintillation crystal
KVI-CART	Kernfysisch Versneller Instituut- Center for Advanced Radiation Technology (Groningen/Netherlands)
$LaBr_3(Ce)$	Lantanum bromide (doped with Cerium): scintillation detector crystal material
LET	Linear Energy Transfer is a measure of the energy transferred to material as an ionising particle travels through it.
LINAC	contraction of the two words *linear* and *accelerator*
LMU	Ludwig-Maximilians-Universität München
LOR	Line of Response: connecting the registered positions of two diametral emitted positron annihilation photons in a PET scanner
LPC	Laboratoire de Physique Corpusculaire (Clermont-Ferrand/France)
LPSC	Laboratoire de Physique Subatomique et de Cosmologie (Grenoble/France)
LSO	Lutetium Orthosilicate: scintillation detector crystal material
LYSO	Lutetium Yttrium Orthosilicate: scintillation detector crystal material
MACACO	Medical Applications CompAct COmpton camera: name of the Valencia Compton camera detector system
Medicyc	Medical Cyclotron (65 MeV protons): first hospital-based cyclotron facility in France for protontherapy, designed and built by CAL Nice.
MediNet	Networking Initiative on Medical Physics within the EU-funded ENSAR2 Integrating Initiative
MGH	Massachusetts General Hospital (Boston/USA)
microTCA (μTCA)	Micro Telecommunications Computing Architecture: Standard for bus-driven electronics, designed for cost-effective, smaller and less demanding applications.
MLEM	Maximum Likelihood Expectation Maximization: iterative method to find maximum likelihood or maximum a posteriori (MAP) estimates of parameters in statistical models, where the model depends on unobserved latent variables
MRI	Magnetic Resonance Imaging is a medical imaging technique using a powerful magnetic field and radiowaves RF pulse of around 40in the 1-100 MHz range.
NaI	Sodium iodide: scintillation detector crystal material
NIRS	National Institute of Radiological Sciences located at Chiba, Japan
OncoRay	Center for Radiation Research in Oncology (Dresden/Germany)
OpenGATE	international collaboration dedicated to (open source) numerical simulations in medical imaging
O-PGI	Orthogonal prompt-gamma imaging: prompt-photon based medical imaging approach developed at LIP Coimbra/Portugal for proton beam range verification
PBS	Pencil beam scanning: modality to deliver the therapeutic particle beam to the patient by scanning the tumor volume with pencil-like individually adjusted particle beams.
PBCT	Proton boron capture therapy: proton beam treatment modality using the proton-boron fusion reaction the generate secondary short-range, high-LET alpha particles for local enhancement of the proton RBE
PCIe	PCIexpress: Peripheral Component Interconnect Express is a standard for the connection of peripheral components with the personal computer.
PET	Positron Emission Tomography is a medical imaging technique using pairs of gamma rays emitted indirectly by a positron-emitting radionuclide.

PET-CT	Positron Emission Tomography and Computed Tomography is a medical imaging device which combines in a single gantry system both a PET and a CT.
PETsys2	PETsys Electronics (Lisbon/Portugal): provider focused on the development and production of gamma ray detectors and related highly-integrated and ASIC-based readout electronics for Positron Emission Tomography (PET) and other applications. TheTOFPET2 ASIC is a new 64 channel chip for the readout and digitization of signals from fast photon detectors in applications where a high data rate and fast timing is required.
PG	Prompt Gamma
PGI	Prompt Gamma Imaging
PGS	Prompt Gamma Spectroscopy
PGT	Prompt Gamma Timing
PGPI	Prompt Gamma Peak Integral
PPS	Particles per second
PSI	Paul Scherrer Institute: largest research institute for natural and engineering sciences in Switzerland, located in Villigen.
PMT	Photomultiplier tube
PMMA	Poly(methyl methacrylate), also known as acrylic or acrylic glass as well as by the trade names Crylux, Plexiglas, Acrylite, Lucite, and Perspex: plastic material commonly used as tissue equivalent phantom material for particle therapy beam and detection system characterization
PRISME	research group at IPNL Lyon that focuses on medical applications of particle physics, i.e. the treatment of cancerous tumors by light ion beams
PTCOG	Particle Therapy Cooperation Group
RBE	Relative Biological Effectiveness is defined as the ratio of a dose of a reference radiation quality to the dose of the test radiation quality required to cause the same biological level of effect, all other conditions being the same.
RF	Radiofrequency (accelerator property, ca. 100 MHz for typical medical cyclotron accelerators)
RUG	Rijksuniversiteit Groningen : University of Groningen (The Netherlands)
SECT	Single-energy computed tomography
Shifting-TOF	A TOF-based mechanism that takes into account the time necessary to stop the incoming proton in the patient.
SiPM	Silicon photomultiplier
SOPB	Spread-Out Bragg peak is an overlap of several pristine Bragg peaks at staggered depths.
SPECT	Single-Photon Emission Computed Tomography
SPCI	single-plane Compton imaging
TOF	Time of flight
TOF-PET	Time-of-Flight Positron Emission Tomography
TBI	Total body irradiation
TPS	Treatment Planning System used in radiation therapy for planning the doses in the tumour and the surrounding healthy tissue (critical organs).
TraDeRa	Transparent Detector for Radiotherapy developed at LPSC Grenoble/France. The detector aims at monitoring the modulated beam ahead of the patient in real-time and without dead zone.

UPTD	University Proton Therapy Dresden
Zn	Abbreviation of the element Zinc
keV,MeV, TeV, ps	Prefix letters together with a unit denote an abbreviated order of magnitude: keV(kilo-eV): 10^3 eV, MeV (Mega eV): 10^6 eV, TeV (Tera eV): 10^{12} eV, ps (pico second): 10^{-12} s

EXECUTIVE SUMMARY

According to the International Agency for Research on Cancer in 2012, there were 14.1 million new cancer cases and 8.2 million cancer deaths, nearly 1 in 6 of all global deaths. Therefore there is evident need of scientific and economic efforts in various cancer treatment modalities, amongst them radiotherapy. The Health Economics in Radiation Oncology project has shown that the need for radiotherapy in Europe is expected to increase by 16% until 2025 [Borras 2016]. Radiotherapy comprises X-ray based radiation therapy and particle or hadron therapy employing accelerated charged particles (mainly protons and carbon ions). In particular, the latter is in the focus of European research teams joining forces in the MediNet Networking Activity within the H2020 ENSAR2 Integrating Initiative.

With this document the members of the radiation detection systems pillar of the MediNet community provide information to the general public on the status and ongoing research efforts in the research field of nuclear physics-related instrumentation used in medicine, especially here focusing on radiation detection instrumentation applied in diagnostics and treatment verification modalities around radiation therapy in cancer treatment. Technological developments from the nuclear physics area, like detector technology (together with related simulation and image reconstruction techniques) as well as particle accelerator science, have gained tremendous importance in the medical field over the past decades. Translation of basic concepts into practical medical applications finally means commercialization, based on a cross-fertilizing interplay between academia and industry. In the present document, a special focus is laid on radiotherapy, which is the overarching topic that unites the interests of the almost 30 research groups from 13 European countries that form the MediNet Networking Activity. The scientifically interested layman is the targeted addressee of the present document, which is organized in the following way:

An introductory section presents the rationale behind particle therapy in comparison to conventional x-ray based radiotherapy and gives a motivation for the need of beam range monitoring due to unavoidable range uncertainties occurring during treatment. As outlined there, the particle range in tissue is associated with considerable uncertainties caused by imaging, patient setup, beam delivery and dose calculation. Reducing the uncertainties would allow for a reduction of the treatment volume and thus for a better utilization of the advantages of the particle therapy modality. The first topical section is dedicated to general aspects of medical imaging techniques, as building the framework for the ongoing R&D activities later on presented. Techniques like Positron Emission Tomography (PET), Single-Photon Emission Computed Tomography (SPECT) and Prompt Gamma Imaging (in its different variants) or (secondary) charged-particle imaging and proton/ion radiography and tomography are presented together with a glimpse on scintillation detector properties as the workhorses of most of the imaging techniques. Together with a prospective paragraph that outlines foreseeable new challenges arising in the field of particle therapy and related radiation detection systems, existing or foreseeable instrumentational needs are introduced that will be addressed in more detail in the second main section.

Here, for the presentation of state-of-the–art studies on instrumentation for medical (imaging) applications the text follows the structure of the MediNet networking activity, where one of its two pillars is dedicated to research on radiation detection instrumentation mainly aimed for application in particle therapy (although with strong synergies into the field of diagnostics). 11 European institutions from 6 countries provide insight into their current work on Nuclear Instrumentation for Medicine, precisely for radiation detection techniques for radiotherapy applications in cancer treatment. Improvements and optimization of established imaging methods like PET and SPECT are presented along with modern approaches on Prompt-Gamma Imaging and imaging using secondary charged particles or new radiation signatures like iono-acoustics.

The documents ends with general concluding remarks.

INTRODUCTION

One of the most fruitful interactions between physics and medicine concerns nuclear physics. Already back in the year 1895, the discovery of X-rays and the density-dependent absorption of electromagnetic radiation was announced by W.C. Röntgen, starting the era of medical imaging. This field became richer and richer during the years, adding more techniques as well as a variety of diagnostic applications. Positron-electron annihilations led to PET (positron emission tomography), single photon emission of specific radioisotopes led to scintigraphy and SPECT (single photon emission computed tomography), and magnetic resonance detection led to MRI (magnetic resonance imaging). Grace to the rapid development of particle accelerator technology also tumor treatment modalities drawing on accelerated charged particles, i.e. electrons as well as hadrons (particles that experience the nuclear force, termed Strong Interaction, like protons or heavier ions) increasingly gained interest, forming the field of radiotherapy.

Nowadays radiotherapy is one of the main treatment modalities for cancer, used in about half of cancer treatments. It delivers ionizing radiation to kill malignant tumor cells, as primary therapy or in combination with surgery or chemotherapy. The goal of therapeutic radiotherapy is to control the tumor by optimizing a dose deposit (amount of energy per unit mass) to eliminate cancer cells or at least stop their development, while minimizing severe side effects like damage to healthy tissue. Currently, radiotherapy is most commonly delivered with external beams of X-rays generated with a linear (electron) accelerator. In contrast, proton (or more general particle or hadron) therapy, in which proton or heavier ion beams (mostly carbon ions) are used instead of X-rays, is a radiotherapy technology that is receiving increasing interest for the treatment of localized tumors. The physical interactions of protons or ions with matter are very different as compared to X-rays, which allows for a superior dose distribution to be created. The depth dose profile is particularly advantageous since the energy deposited in the tissues is low in the ion entrance channel but presents a sharp peak (the Bragg peak) at the end of the path where the tumour is located.

This is illustrated by Fig. 1, where the depth-dose curves both for photons (from a 10 MV linear electron accelerator, dashed curve) and for protons (solid curves) are shown for a realistic irradiation scenario of an extended tumor. Different proton beam energies are applied, whose individual Bragg peaks in combination form a so-called 'spread out Bragg peak' (SOBP) that covers the tumor volume.

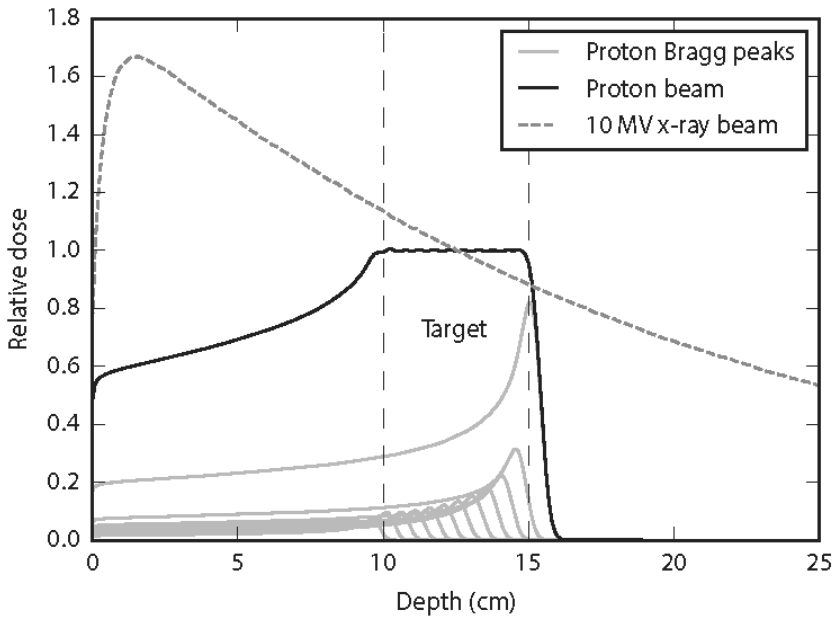

Fig. 1: Comparison of the depth-dose distribution of an X-ray beam and a proton beam in water. The beams target a volume at a depth of 10 cm to 15 cm. From [Verburg 2014a].

In order to fully utilize the potential advantage when using protons or ions, the range of particle beams in patients needs to be predicted as accurate as possible in the treatment planning and delivery process. An improper quantification of safety margins can have more severe consequences in hadron therapy than in photon therapy. Margins underestimating uncertainties in photon therapy might cause under-dosage of the tumor. In particle therapy, such an underestimation may cause part of the tumor not receiving any dose due to a potential shift of the sharp distal dose fall-off. Uncertainties in the exact position of the distal dose gradient arise from a) organ motion, b) setup and anatomical variations, c) dose calculation approximations, and d) biological considerations. At the Massachusetts General Hospital (MGH), treatment planning assumes an uncertainty in the proton beam range of 3.5% of the range plus an additional 1mm. Other centers follow similar margin recipes. For example, the MD Anderson Proton Therapy Center in Houston, the Loma Linda University Medical Center, and the Roberts Proton Therapy Center at the University of Pennsylvania all apply 3.5% + 3mm while the University of Florida Proton Therapy Institute uses 2.5% + 1.5mm.

The concept of safety margins (up to 10 mm around the tumor target) actually prevents *de facto* a full exploitation of the therapeutic potential of hadron therapy. This concept is illustrated in Fig. 2, showing the safety margin of 1.5σ of the expected beam range distribution placed around the distal edge of the target volume. A separation of 2σ between the mean end of the beam particle range and a downstream located organ at risk (OAR) is also shown. If this OAR is located closer to the target it may prevent an irradiation of the target volume in the displayed direction.

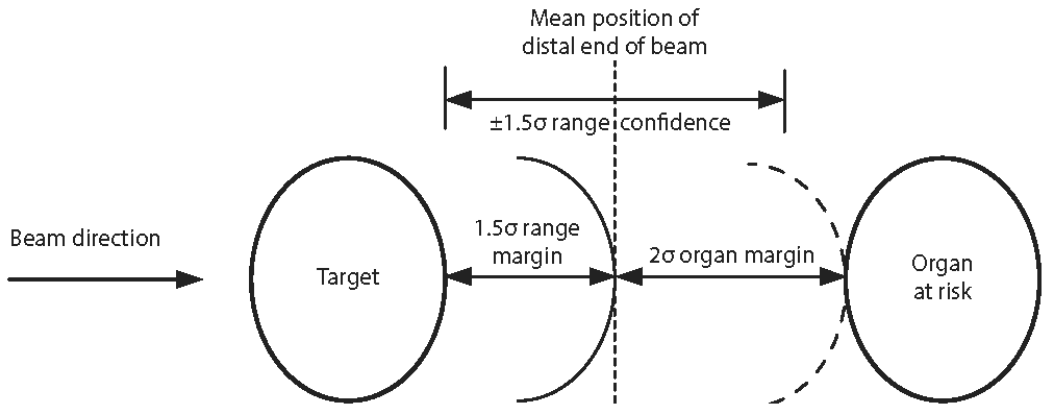

Fig. 2: Illustration of typical range margins that ensure that a proton or ion beam that delivers a uniform dose is robust against range uncertainties. The distal dose surface is positioned at a distance from the target of 1.5σ of the expected range distribution. A separation of 2σ between the mean end of range and a downstream organ at risk is also shown. If the organ at risk is located closer to the target, it may not be clinically possible to irradiate with a particle beam in this direction. From [Verburg 2014a].

Uncertainties could be better addressed and, potentially, safety margins reduced if routine *in-vivo* range monitoring and verification would be available in particle therapy facilities. Therefore, as will become obvious in Section 2, large efforts are devoted to realizing such a precise and in-vivo particle beam range monitoring. Since all that is pursued in the framework of the continuous quest for optimizing medical imaging technologies, the next section is devoted to introduce those imaging techniques being most relevant for the work ongoing in the research teams forming the Radiation Detector Development pillar of the MediNet initiative.

SECTION 1: GENERAL ASPECTS OF MEDICAL IMAGING MODALITIES

'Medical Imaging' refers to several different technologies that are used to view the human body in order to diagnose, monitor, or treat medical conditions. Each type of technology gives different information about the area of the body being studied or treated, related to possible disease, injury, or the effectiveness of medical treatment.
Medical imaging using radioactive isotopes makes use of two distinct types of "camera". Isotopes decaying by the emission of a positron (β^+ emitters) are imaged by a positron-emission tomograph (PET scanner). In tomography, a 3-dimensional image of an object is obtained by combining 2-dimensional images taken at different angles around the object. Radioisotopes emitting gamma rays are imaged by so-called gamma cameras. Such a camera is used to take 2-dimensional images and, when positioned on a rotating gantry, allows for tomographic imaging (SPECT: single photon emission computed tomography, Compton Imaging, Prompt-Gamma Imaging). Photon emission can take place following radioactive tracer injection into the body in the context of diagnostics performed in Nuclear Medicine or as quality monitoring modality accompanying irradiations with charged particle beams (protons, ions) in hadron therapy for tumor treatment. Prior to presenting ongoing technological developments around nuclear (radiation detection) instrumentation, introductory remarks will be made on the different radiation-related medical imaging techniques which are in the focus of the participant groups of the MediNet Networking Activity.

Positron Emission Tomography (PET)

Positron-emission tomography (PET) is a functional (as opposed to anatomical) imaging technique used both in nuclear medicine and particle therapy. The detector system registers coincident pairs of gamma rays emitted almost under 180 degrees from the annihilation of the positron emitted from a radionuclide decaying via β^+ radioactivity. In nuclear medicine the most commonly used radioisotope is fluorine-18, which is introduced into the body on a biologically active molecule called a radioactive tracer. Three-dimensional images of tracer concentration within the body are then constructed by computer analysis. In particle therapy, imaging of β^+ emitters (like ^{11}C), which are generated online during tumor irradiation, is performed either directly after or even during therapeutic irradiation [Parodi 2016]. In modern PET-CT scanners, three-dimensional imaging is often accomplished with the aid of a CT X-ray scan performed on the patient during the same session and in the same machine.

Nowadays a typical state-of-the-art commercial clinical PET scanner consists of a few ten thousand small scintillation crystals that individually detect the 511 keV positron annihilation photons emitted by the radiotracers injected into the patient's body. The coincidently registered detection times are measured very accurately, with a precision of about half a billionth of a second. Data rates are large: typically of the order of a million events per second. Sophisticated algorithms allow to reconstruct 3D images out of the huge recorded data set. Images with a spatial resolution of about 4 mm are obtained. A whole body scan with the ^{18}FDG tracer, one of the most common PET procedures, takes about 15 minutes.
The scanner bore of about 80 cm diameter is determined by the typical patient size, the axial length of 20-25 cm is a matter of limiting the costs. Nowadays, all PET scanners are combined with an X-ray CT scanner for a quick, easy and accurate determination of the attenuation correction needed for quantitative imaging (due to interactions of the emitted photons in the patient prior to reaching the detectors). Scanners come with a collection of sophisticated data and image analysis options for specific scan procedures and clinical investigations. Ease of use and integration in the clinical workflow are well-developed important features. In addition, modern PET scanners also exploit the timing information provided by fast scintillation materials: the difference of the time-of-flight for the coincident 511 keV positron annihilation photons (called coincidence resolving time, CRT) is used to restrict the positron annihilation positron along the line-of-response defined by the two diametral responding detector

crystals. Nowadays CRT values of 500 ps are used in clinical settings, with values as low as 100 ps already realized in the laboratory [Schaart 2010].

Single Photon Computed Tomography (SPECT)

Single-photon emission computed tomography (SPECT) is a tomographic imaging technique using gamma rays, able to provide true 3D information. This information is typically presented as cross-sectional slices through the patient, but can be freely reformatted or manipulated as required. The technique requires delivery of a gamma-emitting radioisotope into the patient, normally through injection into the bloodstream.
A SPECT scan monitors the level of biological activity at each place in the analyzed 3D region. Emissions from the tracer radionuclide indicate the amounts of blood flow in the capillaries of the imaged regions. In the same way that a plain X-ray image is a 2-dimensional (2D) view of a 3-dimensional structure, the image obtained by a (SPECT) gamma camera is a 2D view of the 3D distribution of the radionuclide. The most frequently used SPECT radiotracer is ^{99m}Tc (half-life 6 hours), emitting photons with an energy of 140 keV.
The physical characteristics of SPECT scanners have not changed much over the past few decades. The originally used scintillation material, NaI, remains adequate for the task, mainly because sensitivity and image resolution are largely determined by the collimator positioned in front of the detector. Collimators are rather simple mechanical devices that have been optimized quite a while ago. Nevertheless, SPECT scanner developers have made use of the rapid progress in electronics and computation, improving, e.g., the ease of use, stability and reliability.
Recently proposals have been put forward to translate detector concepts based on electronic instead of mechanical collimation, as will be detailed later on.

Prompt Gamma Imaging (PGI)

Prompt Gamma Imaging (PGI) is one of the imaging techniques using secondary radiation generated during therapeutic irradiation of tissue in order to monitor the range of the particle beam, namely the Bragg peak. The PGI method utilizes a dedicated gamma camera to produce an image of the proton (or ion) tracks by measuring a 1-dimensional (1D) profile of multi-MeV prompt gamma rays transmitted through the patient after emission by excited nuclei along the particle beam path. Prompt gamma imaging has been proposed as a superior method to Positron Emission Tomography (PET) for range verification, with the potential to achieve 1 mm uncertainty in the positioning of the Bragg peak within the patient [Moteabbed 2011]. PGI allows real-time range verification and does not suffer from biological washout or motion effects. In addition, a significantly higher PG production and closer correlation with dose profiles due to higher cross-sections makes it more attractive than PET [Martins 2017].
Several techniques for such imaging have been proposed, each exploiting a different aspect of the prompt photon emission. A comprehensive overview is given in [Krimmer 2018], key elements are shortly described below to introduce later on presented reports on currently ongoing state-of-the-art research and development activities in the MediNet participant groups (Sect. 2).

Prompt gamma spectroscopy: Identifying discrete γ-ray lines, attributed to specific nuclear transitions originating from excited nuclear states being populated in the interaction of the therapeutic particle beam with the organic material of the irradiated tissue, can provide several benefits to improve the accuracy and sensitivity of therapeutic particle beam range verification. First, each of these discrete γ-ray emissions has a unique correlation to the proton (ion) energy, and nuclear reaction cross sections may be used as prior knowledge in the range verification procedure. Second, using the prompt γ-ray production cross sections, the concentrations of the target nuclei for the particle-beam induced reactions in the irradiated tissue may be estimated based on the specific γ-ray emis-

sions, which can make beam range verification more robust if the particle beam stops in tissue with an uncertain composition [Verburg 2014].

Prompt gamma timing: The idea behind PG-Timing (PGT) proposed by Golnik et al. [Golnik 2014] is to retrieve the beam range by means of time position and width. Proton or ion beams entering material cause the emission of prompt gamma-rays along their path, until they are stopped. The transit time for protons/ions with a range of 5-20 cm is on the order of 1-2 ns. As the transit time depends on the range, this information is reflected in the width of prompt gamma-ray TOF distributions. With the technique of PGT range shifts of 5 mm in homogeneous targets can be detected for clinically relevant doses, this value is reduced to 2 mm for higher statistics [Hueso-Gonzalez 2015].

Prompt-Gamma Peak Integral: The prompt-gamma peak integral (PGPI) method proposed by Krimmer et al. [Krimmer 2017] makes in addition use of the peak integrals of prompt gamma-ray time-of-flight (TOF) distributions to verify the beam position, the range and thus the energy deposited in the patient, therefore approaching in vivo dosimetry. TOF provides a possibility for a discrimination of the prompt gamma-rays produced in the target (patient) from those generated in the beamline, e.g. in the nozzle. The general goal is to detect deviations from the prescribed treatment and in particular to avoid severe overdosage.

Compton imaging: In comparison to gamma camera systems with passive collimation (slit/multislit camera, knife-edge camera) the use of electronic collimation, i.e. Compton cameras, has the general advantage of a higher detection efficiency. Compton cameras for medical imaging have first been proposed in [Everett 1977]. The principle is to use successive interactions (two or more) of the incident photons in segmented detectors. From the interaction points in the detectors and the deposited energies the direction of the incident photon can be restricted to a cone, via the application of Compton kinematics. The vertex of the photon generation is then obtained via the superposition of multiple cones. An advantage of the Compton cameras is, that in principle 3-D information is available. This type of camera is also well adapted for prompt gamma-ray detection, because in the energy range of several MeV Compton scattering is the dominant process. The simplest realization of a Compton camera requires two detection stages, a scatter detector and an absorber. As for the monitoring purpose during hadron-therapy the energy of the induced prompt gamma-ray is a priori not known, this type of cameras requires a total absorption of the scattered photon in the absorber in order to kinematically reconstruct the event.
As will be shown in Sect. 2, extensive efforts are devoted within the MediNet activity to advancing this promising modality of Prompt Gamma Imaging.

Charged particle imaging

During irradiation with primary ions heavier than protons, lighter projectile fragments are produced in collisions of the incident ions with nuclei of the irradiated tissue. Some of these light fragments have enough energy to leave the patient and can easily be detected. A reconstruction of the trajectory of the emerging charged particles and the intersection with the impinging ion path gives the point of ion– nucleus interaction. By means of a comparison between simulated and measured vertex distributions, the range of impinging ions can be verified. This method is also known as interaction vertex imaging, and several MediNet research teams work towards this alternative to photon-based imaging.

Ion radiography and tomography

Ion radiography enables the direct measurement of the residual range of high-energy, low-intensity ions traversing the patient. It may replace X-ray radiography to produce low dose, high density resolution images of the pa-

tient at the place of treatment. In terms of pre-treatment verification, the method can also be used to validate in vivo the treatment planning range calibration curve deduced from the X-ray CT, which currently introduces the larger source of range uncertainties due to different physical processes of ion and photon interaction. Tomographic extension of radiographic imaging can enable volumetric images, providing a direct measurement of the ion stopping power ratio relative to water. Due to the weak energy dependence of the stopping power ratio, these images obtained at higher energies than for therapy can be used as a patient model in treatment planning, again eliminating the range uncertainties connected to the usage of calibrated X-ray CT images. Spatial resolution of the method is limited by multiple Coulomb scattering in the patient, which is more pronounced for protons than for heavier ions. However, 1 mm is anticipated to be achievable, even for the more scattering protons. New prototypes are currently under development both for protons and carbon ion beams.

Ionoacoustics

When penetrating a medium, ions mainly lose energy in electronic collisions, resulting in localized heating and a thermal expansion, which generates thermoacoustic emissions detectable with acoustic transducers. Being the thermoacoustic emission naturally enhanced at the maximum of ion energy deposition (so-called Bragg-peak), time-of-flight (TOF) measurements in combination with knowledge of the speed of sound in the traversed medium can enable recovery of the ion range. Especially in combination with morphological ultrasonography, this so-called “ionoacoustics” could offer a compact and cost-effective modality for real-time in-vivo verification of the beam range, co-registered to tissue anatomy, at least for suitable indications of feasible sonic access [Parodi 2015, Assmann 2015, Lehrack 2017].

Radiation detector developments

Despite the excellent performance reached by radiation detectors for medical imaging over the years, mainly for the purpose of being applied in PET or SPECT scanner systems, there is room for improvement that will also allow for non-standard use of, e.g., PET technology, such as in-beam measurements during particle therapy sessions, or PET imaging based on β^+-γ coincidence measurements. Research is being carried out worldwide in order to improve all relevant aspects that contribute to the overall performance of a PET scanner: detection efficiency, spatial resolution, depth of interaction measurement, time resolution, compactness, MR compatibility, speed, power consumption.

Scintillation crystals are the workhorses in all kinds of gamma cameras used for medical imaging as discussed in the context of this document. In order to be used as a primary photon converter for a PET (fixed photon energy) and a SPECT (wide photon energy range) or prompt-gamma imaging (high photon energies) detector, a scintillating crystal must meet the following requirements:

- high density (i.e., high conversion efficiency);
- high light yield (related to the energy and time resolution);
- short rise time to optimize the time resolution.

The figure of merit that summarizes the suitability of a crystal is usually defined as: $\eta \sim \varepsilon^2 \sqrt{N/\tau}$, with ε, N, τ related to the crystal density, light yield and decay time, respectively. In addition, the technology must provide uniform crystals at a low (acceptable) cost.

The state of the art for PET/SPECT scanners is a set of inorganic crystals, whose properties are summarized in Table 1. LSO and LYSO are the currently best choice for scanners that also perform the Time-Of-Flight measurement. However, the search for new materials that would better meet the requirements for a more efficient and

time performance scanner has not stopped and has been also pursued in the framework of MediNet participant groups.
As an optimal timing resolution is related to the photon counting statistics, it requires the capability to trigger at very low threshold, with the performance limit being reached when counting single photons. When these conditions are met, a high light yield and a short rise-time of the scintillating light allow the best measurement of the interaction time, with the possibility to approach values of about or even below 100 ps.

Table 1. Properties of most used scintillator materials in PET and SPECT [Adapted from R. Lecomte, Eur. J. Nucl. Med. Mol. Imaging. 36, Suppl. 1 (2009): S69–S85.]

	NaI	BGO	GSO	LSO	LYSO	LGSO	LuAP	YAP	$LaBr_3$
Light yield 10^3 ph/MeV	38	9	8	30	32	16	12	17	60
Primary decay time	250	300	60	40	41	65	18	30	16
ΔE/E (%) at 662 keV	6	10	8	10	10	9	15	4.4	3
Density (g/cm^3)	3.67	7.13	6.71	7.35	7.19	6.5	8.34	5.5	5.08
Effective Z_{eff}	50	73	58	65	64	59	65	33	46
1/μ @ 511 keV (mm)	25.9	11.2	15.0	12.3	12.6	14.3	11.0	21.3	22.3
PE (%) at 511 keV	18	44	26	34	33	28	32	4.4	14

New challenges

Increasingly, multi-modality imaging (meaning the combination of SPECT or PET with X-ray CT) is used in order to show both the functional molecular processes taking place in the body (via SPECT or PET) and the anatomical location in which they are happening (via CT) so that, for example, a tumour can be detected using PET imaging and located using CT in a PET/CT scanner. PET/CT was introduced more than 15 years ago and multi-modality is standard for SPECT and PET machines which are now on sale.
In recent years also the combination of PET (and SPECT) with Magnetic Resonance Imaging (MRI) has found its way into clinical practice. The benefits are to reduce the radiation dose by eliminating the CT scan, and the possibility to use functional MRI as well as simple anatomical MR scans (so that blood flows, for example, can be detected). However, this is technically more difficult because typical SPECT and PET scanners traditionally use scintillators with photomultipliers (PMT) which are incompatible with the intense magnetic fields in modern MR scanners. The rotating gantries used in PET and SPECT can also be affected by the MR magnetic field. Conversely the PET detectors must not affect the sensitive MR scanner operation either by perturbing the field or introducing electrical noise. Technology from nuclear physics detector systems is used to overcome the magnetic incompatibility by replacing the PMT photosensor with semiconductor light sensors (APDs or SiPMs) or to replace scintillators by semiconductor detectors.

Moreover, new challenges already appear at the horizon which are linked to upcoming novel tools that are (or soon will become) available in the field of ion acceleration. Ongoing remarkable developments and their implications for therapy can considerably change the scenario of future treatment modalities. These include, in particular, the development of laser-driven ion beams (e.g. pursued at the GSI/FAIR TNA facility), the use of high-intensity beams, e.g. enabling the “Flash” irradiation scheme, high dose-rate ion beams, biologically-enhanced

treatment modalities, radioactive beams, ions different from hydrogen and carbon and spatial and temporal fractionation, using, e.g., mini-beams or micro-beams from synchrotron radiation. Also the Boron Neutron Capture (BNCT) therapy modality emerges into the focus of radiobiological and dosimetry studies, e.g. at the NLC Transnational Access laboratories in Warsaw and Cracow.
Part of the instrumentation currently available in ion-beam therapy is not compatible with these new irradiation modalities (in particular the high beam currents) and novel techniques and methodologies should be investigated to provide the required dosimetry and quality assurance and, possibly, to give immediate feedback on the accuracy of the irradiation with completely new online tools (like, e.g. iono-acoustics or very short-lived PET isotopes).
Further developments will address the combination and/or comparison of several modalities, the use of fast timing techniques for particle and gamma detection, the development of fast data acquisition systems or the integration of simulated secondary radiation distributions into QA systems, which requires fast simulations associated to treatment plans. Also neutron spectra generated in treatment facilities and posing potential radiological risks will be addressed, so far given only scarce attention. Given the wide energy spectra, accurate measurements are not trivial and MediNet experts can make important contributions.

Following these basic introductory remarks, the next section illustrates the broad scope of currently ongoing research and development on nuclear radiation detection systems applied for medical physics both in nuclear medicine and radiation therapy. It provides an overview of currently pursued activities on Radiation Detection systems conducted by the participant groups of the European Networking Initiative ‘MediNet’, and here in particular its pillar ‘Task 1’ that brings together the leading European groups working on radiation detection systems (mainly) for radiotherapy.

SECTION 2: SPECIFIC RESEARCH ACTIVITIES OF MEDINET (TASK 1) PARTICIPANTS IN THE FIELD OF NUCLEAR INSTRUMENTATION FOR MEDICAL PHYSICS

The European endowment with presently 23 proton (or C ion) particle beam treatment facilities in operation (representing about one third of the present worldwide capacity) is rooted in a dense and active network of research groups at various institutions. They provide continuous support and optimization for particle therapy and auxiliary technologies, amongst them radiation detection techniques for diagnostics and treatment quality verification. The MediNet networking initiative comprises the leading European groups in the field, actively driving progress in the area of photon and particle detection techniques for medical imaging. The following section is dedicated to an overview of the broad scope of presently ongoing R&D activities in the member institutions of the MediNet pillar working on radiation detector developments for radiation therapy.

External beam radiotherapy aims at destroying tumor cells by using beams of ionizing radiation from sources external to the patient. Beams of ions such as protons or carbon ions deliver a peak of radiation dose, the Bragg peak, in a small region at the end of their range, and a very small dose beyond this peak. This in principle allows a more accurate irradiation of a tumor while reducing the integral dose to healthy tissue as compared to radiotherapy using high energy photon beams.

The advantageous dose deposition possible with beams of protons or ions is in practice not yet fully accomplished due to uncertainties in predicting, during treatment planning, the location of the Bragg peak in the patient and the lack of in-vivo dose delivery verification methods during irradiation. These shortcomings are presently taken into account via conservative treatment planning (e.g. employing relatively large safety margins around the tumor and avoiding beam directions pointing at critical organs), unavoidably leading to non-optimal treatment plans.

Several options are pursued, drawing on secondary radiation like prompt photons, charged particles or ultrasonic signals. One route employs the concept of an electronically collimated gamma camera, where the kinematics of Compton scattering, i.e. the scattering between an impinging photon (e.g. arising from nuclear interactions of the treatment beam with the organic constituents of patient tissue) and electrons of the radiation detector material can be exploited to reconstruct the position of the photon origin. With a clear correlation between the dose deposition of the treatment beam and the emission profile of prompt secondary photons, this 'prompt gamma imaging' using a so-called Compton camera is a promising way to address the quest for reducing safety margins in particle therapy. Moreover, this technique can also be used to optimize the performance of diagnostics modalities like PET (via a combination of PET scanners with one or more Compton cameras to register triple coincidences emerging from specific β^+ decaying radioisotopes) or SPECT (replacing the traditional mechanically collimated Anger-type gamma camera by an electronically collimated Compton camera). The following paragraphs describe research activities of MediNet groups working in this field of instrumentation development.

LMU Munich/Germany: (P.G. Thirolf, K. Parodi et al.)

Traditionally a Compton camera consists of a scatter and an absorber component, both of them allowing for the determination of the photon interaction position and registering the amount of deposited energy. Exploiting the fundamental principles of energy and momentum conservation, equations can be derived that describe the kinematical relations governing the scattering of a primary photon in the scatter component and to quantify the (energy dependent) scattering angle of the photon. This angle spans a cone (the 'Compton cone'). Fig. 3 illustrated this situation: the line between the first (scattering) and second (absorption) interaction determines the axis of the cone, whose opening angle θ is given by the Compton scattering formula derived from the kinematical relations. From an individual photon interaction event the origin of the photon can only be correlated with the surface of this cone, however, if many photons are registered the intersection of their Compton cones will allow for a

reconstruction of the initial source position. The conventional design of the Compton camera with a single scatter plane requires full absorption of the remaining scattered photon energy in the subsequent absorber component. However, Compton scattering may occur there as well, potentially leading to a scattered photon escaping from the absorber volume, thus resulting in an incomplete absorption of the primarily scattered photon and thus a wrong energy input into the Compton formula. These events will either blur the source reconstruction or have to be discarded, thus reducing the reconstruction efficiency. The Compton camera prototype developed at LMU Munich and presently under commissioning aims at mitigating this deficit by enabling a tracking of not only the Compton scattered photon, but also of the Compton electron, as indicated in the left panel of Fig. 3 [Thirolf 2013, Thirolf 2014]. Therefore the scatter component consists of a stack of thin position sensitive detectors (here: six double-sided silicon strip detectors with 0.5 mm thickness, 50x50 mm^2 active area and a fine segmentation of 128 strips per side). Tracking the Compton-scattered electron provides an independent kinematical path and therefore allows for reconstructing also incompletely absorbed scattered photon events. Moreover, the Compton cone reduces to an arc segment in this case, as illustrated in Fig. 3. The right panel of Fig. 3 schematically shows the layout of the LMU Compton camera prototype: besides the six scatterer layers, the absorber consists of a monolithic scintillator block (50x50x30 mm^3), either from $LaBr_3$(Ce) or $CeBr_3$, read out by position-sensitive multi-anode photomultiplier tubes. These materials were chosen due to their excellent energy and timing properties ($\Delta E/E \approx$ 3.5-4.5% at 662 keV and $\Delta t \approx$ 270 ps) [Aldawood 2015].

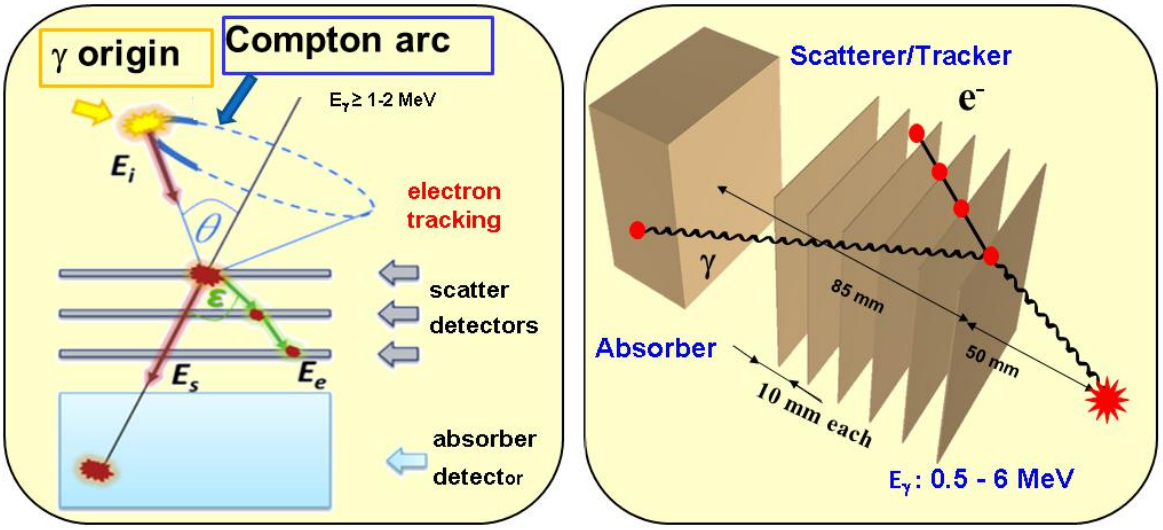

Fig. 3: Operational principle of the LMU Compton camera prototype with electron tracking capability (left) and schematic layout of the scatter and absorber component.

A challenge of this geometrical layout is the need to derive the photon interaction position from a monolithic scintillator. This is achieved by applying the 'k-nearest neighbor algorithm' (k-NN), that is based on a large reference library of 2D light amplitude distributions acquired by scanning the scintillator front surface with a tightly (1 mm) collimated photon source (^{137}Cs: 662 keV or ^{60}Co: 1172 and 1332 keV). Scanning the detector in 0.5 mm steps and registering a few hundred photopeak events for each irradiation position allows for a comparison of a later unknown photon event with each of the library entries. A selectable number of *k* closest matching 2D light distributions from the (8x8 or 16x16 segmented) multi-anode photomultiplier is then retrieved. Since the irradiation positions of the *k* events are known, after smoothing the maximum of their 2D distribution will be identified with the desired interaction position of the absorbed photon. Systematic studies were performed for $LaBr_3$(Ce) and $CeBr_3$ with both photon sources and various parameters of the reconstruction algorithm (events per position,

number *k* of 'nearest neighbours'). Fig. 4 shows two maps of resulting 2D light amplitude distributions, where each of the 16x16 subsets corresponds to the 2D light distribution seen by a 16x16 segmented multi-anode PMT (Hamamatsu H9500). In each case the collimated photon source (left panel: ^{137}Cs: 662 keV, right panel: 1332 keV from ^{60}Co) was moved in steps of 3 mm from the upper left to the bottom right corner. For the final reference library this scan was performed with a step size of 0.5 mm in both directions, resulting in about 10^4 irradiation positions [Thirolf 2016].

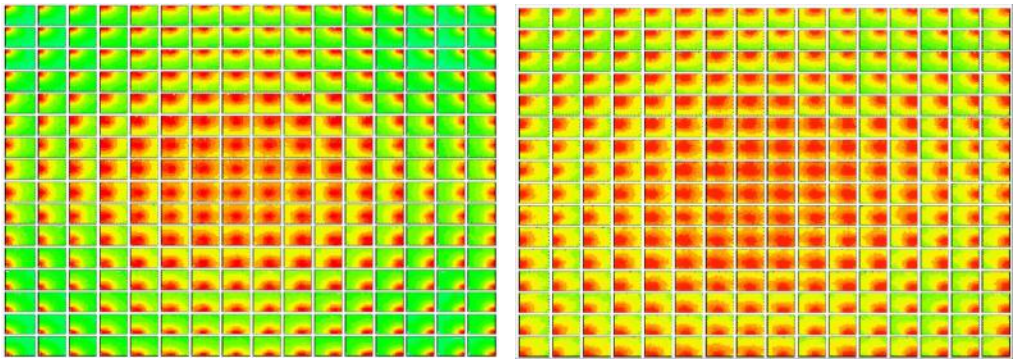

Fig. 4: 2D light amplitude distribution maps obtained from the irradiation of a $LaBr_3$(Ce) scintillator read out by a 16x16 fold segmented multianode photomultiplier with a 1mm-collimated photon source (left: ^{137}Cs, right: ^{60}Co) in steps of 3 mm in x and y direction. The sources were consecutively moved from the upper left to the lower right corner of the detector, each subset reflects the 16x16 (x,y) pixel readout from the PMT segments.

A quantitative analysis of the achievable spatial resolution as a function of the photon energy results in the plot shown in Fig. 5: it turns out that (due to the light collection statistics), a 64-fold PMT segmentation provides equal or even better spatial resolution than a finer granularity of 3x3 mm (256-fold segmentation), thus allowing for a considerable reduction of the complexity of the signal processing electronics. While for $LaBr_3$(Ce) an energy-dependent improvement of the spatial resolution is found with sub-3 mm resolution at ^{60}Co energies (2.7(1) mm), this result is almost independent of the photon energy reached for the $CeBr_3$ scintillator (with an optimum value of 2.6(1) mm at 1.3 MeV). The considerably better spatial resolution at 662 keV for $CeBr_3$ (2.7(1) mm vs. 3.4(1) mm) is most likely due to the absence of internal radioactivity in this material, leading to additional blurring in the case of $LaBr_3$(Ce). A remaining challenge will be to confirm this result also for the multi-MeV range of interest in prompt-gamma imaging (requiring a well-collimated, intense, multi-MeV photon beam) [Aldawood 2017, Liprandi 2017].

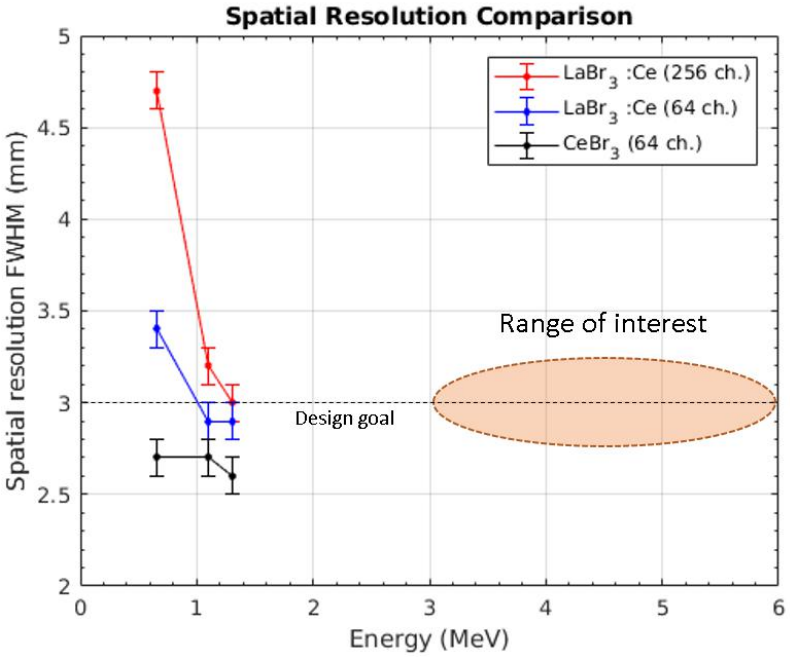

Fig. 5: Spatial resolution of monolithic $LaBr_3$(Ce))(red, blue) and $CeBr_3$ (black) scintillators as a function of the incident photon energy. Results for the $LaBr_3$(Ce) case are compared for 2 photosensor (multi-anode PMT) granularities (8x8 and 16x16 segments, respectively).

In the ongoing quest to optimize the performance of the camera system, in particular in view of a later translation into clinical operation, also alternative components are evaluated: $CeBr_3$ is being studied as almost as high performant, yet more cost-efficient scintillator material with the additional advantage of exhibiting no intrinsic radioactivity. In order to enable an application of the Compton camera also in an environment with magnetic fields (like in PET/MR devices or in a particle treatment room close to the beam delivery nozzle with potential magnetic stray fields of bending magnets), magnetically insensitive silicon photomultipliers are studied as alternatives to photomultiplier tubes. Fig. 6 shows such an array of 3x3 mm^2 SiPM pixels (KETEK) that is envisaged as photosensor for the absorber component of the Compton camera.

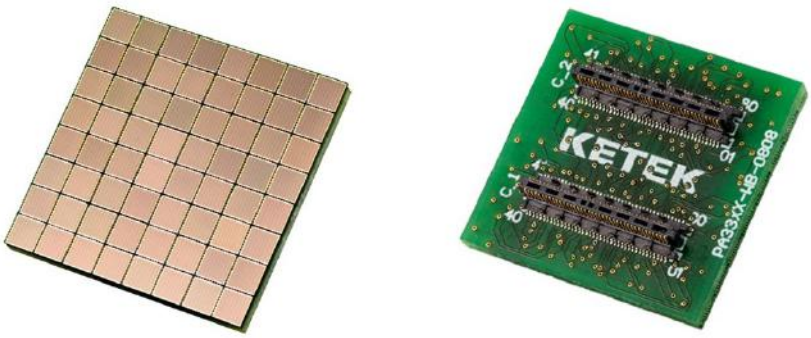

Fig. 6: Photograph of an SiPM array under study as potential alternative as photosensor for the readout of the absorber component of the Compton camera.

In parallel also efforts are ongoing to minimize the demand for computational time and resources for source reconstruction by using machine learning algorithms.

Finally, Compton camera based imaging can also be used to improve the performance of PET by allowing the use of a new class of PET isotopes, so far disregarded for imaging: β^+ emitter may decay to excited states in the daughter nucleus, which subsequently de-excites via the emission of a prompt photon. So in total this β^+ decay will generate 3 photons, which can be detected in coincidence, e.g via a PET detector assembly for the two positron annihilation photons, while the track of the third prompt photon is registered by a Compton camera [Lang 2012, Lang 2014, Thirolf 2015] This allows for reconstructing the primary photon origin through the intersection of the line-of-response of the 511 keV annihilation photons with the track of the prompt photon, in principle within one single event. This avoids or at least reduces the blurring effect that originates from the diffusion of the positron during its thermalization prior to annihilation and results in a considerably improved sensitivity of the so-called γ-PET (or triple-γ PET or Whole Gamma Imaging) imaging modality. It can be applied either for improved PET diagnostics conditions, e.g. using the $\beta^+\gamma$ decaying isotope ^{44}Sc (third photon energy 1.157 MeV), or in a hybrid scenario in particle therapy, where online produced $\beta^+\gamma$ emitter like ^{10}C or ^{14}O can be imaged in addition to the prompt multi-MeV photons from the direct beam interaction with tissue.

IFIC (CSIC-UVEG), Valencia (Spain) : (G. Llosá, J.F. Oliver, A. Ros et al.)

The IRIS group at IFIC Valencia is developing a three-layer Compton telescope (CT) for treatment monitoring in ion beam therapy. The system is composed of three $LaBr_3$ scintillation detector planes coupled to SiPM arrays. (Conventional) two-layer Compton cameras can be employed when the photon energy is known or when it is low, so that the second detector can fully absorb the photons. Since this is not the case in this application, a three-layer version is an interesting option, given that three distinguishable interactions in known order allow the photon energy to be determined. However, this comes at the price of a much lower efficiency than the double-interaction solution. The aim of the IRIS group at Valencia is to combine two- and three-interaction events and to estimate the initial photon energy through the data analysis process in the two-interaction case. $LaBr_3$ crystals have a high Compton scattering probability and a good energy resolution, and their operation coupled to silicon photomultipliers (SiPMs) results in a simple and compact device, well adapted to a clinical environment.
The first prototype of MACACO (Medical Applications CompAct COmpton camera) was fully characterized in the laboratory and during in beam tests demonstrating the feasibility of the proposed technology and identifying the main limitations [Munoz 2017, Munoz 2018, Solevi 2018]. A second prototype, MACACO II, is currently under development to improve performance. The first step has been the replacement of the SiPM arrays employed as photodetectors by newer versions with better performance, with the aim of improving the detector energy resolution. New $LaBr_3$ crystals have been acquired, matching the size of a single SiPM array with 8x8 pixel elements instead of the four arrays per detector previously employed. The external dimensions of the device are 25.8x25.8 mm^2. Each of the 64 pixels of the SiPM array is 3x3 mm^2 in size [Barrio 2017].

The new detectors have been assembled on a printed circuit board (PCB) containing the crystal coupled to the photodetector and the readout ASIC. A temperature sensor is attached to the back of the PCB in order to monitor the temperature of the detector plane. The $LaBr_3$ scintillator crystals have 5 mm thickness. Two detectors have been assembled and tested, and a third one is under development. Meanwhile, one of the old detectors is employed for the three-layer tests. The readout system is a custom-made data acquisition board that operates the ASIC. A coincidence board allows us to measure events in time coincidence between any two or all three planes simultaneously.
A characterization of the new detector modules was carried out, achieving an energy resolution of 6% FWHM for a point-like ^{22}Na source (511 keV peak) in routine operation, compared to the 7.5-8% previously achieved. Posi-

tion determination response was shown to be linear in the central area of the detector and an average spatial resolution of 1.2 mm FWHM was measured.

Particular emphasis has been put forth in the improvement of the image reconstruction codes. Image reconstruction is the process that translates the raw measurements registered by the system into fully tomographical images. From a mathematical point of view, it is essentially an inverse problem, where we are interested in determining the distribution of a signal that produced the registered measurements. To this end, detailed models of the physics involved in the process of the detection are necessary. Such physical models of the image formation process in a two layer CT have been recently developed, also allowing to obtain the sensitivity of the device. Technically, the sensitivity in a given point of the space indicates how probable it is that an emission in that point ends up being detected by the system. The knowledge of the sensitivity is very important to obtain valid images also in regions which are not directly below the Compton telescope, i.e. in regions where the device is less sensitive. With these developments, we have been able to improve the quantification of the source intensities. In addition, the relative intensities of photon calibration sources located in different positions of the field of view (FoV) are properly reconstructed. The newly developed sensitivity model has been compared to simpler ones available in the literature and in all scenarios it has outperformed them, especially for 'low-coverage' configurations, where the second plane is moved away from the first one to enhance the spatial resolution of the imaging system [Munoz 2018a].

The Compton telescope composed of the two new planes and the improved reconstruction code has been tested with point-like sources located in different positions of the field of view, along the longitudinal and transversal directions. Also, a ^{22}Na array of 37 point-like sources was imaged showing the significantly improved imaging capabilities of the new system with respect to the previous prototype (Fig. 7). Simulations have also been carried out with the simulation toolkit GATE, matching the experimental results and are being used to investigate the system capabilities in optimized conditions.

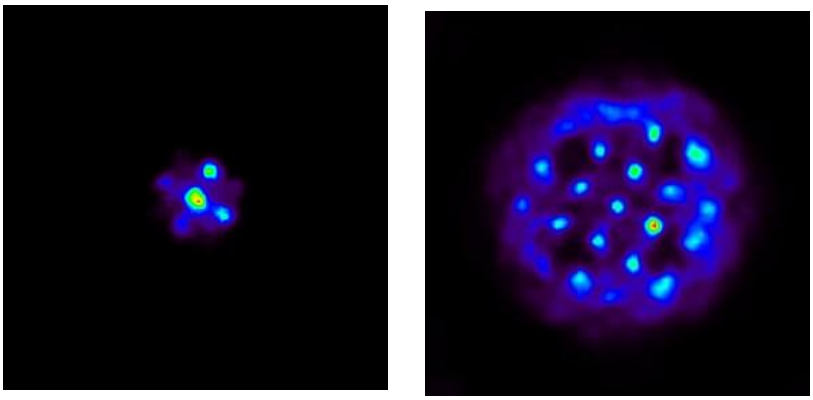

Fig. 7: Image of a ^{22}Na array of 37 point-like sources with MACACO II not applying (left) and applying (right) our sensitivity model in the image reconstruction

The device has also been tested in accelerator facilities. Initial beam tests were carried out at CNA (Sevilla) with a proton beam of 18 MeV impinging on a graphite target and producing 4.4 MeV gamma rays. The results allowed for a successful reconstruction of two target positions separated by 5 mm.

The second test beam with MACACO II was held at KVI-CART with the AGOR cyclotron producing a 150 MeV proton beam. A cylindrical PMMA target, 60 mm in diameter and 160 mm in length, was used (Fig. 8). Preliminary analysis results show prompt-gamma energy spectra as expected for these proton energies. The analysis of these data is ongoing, with the aim of reconstructing the Bragg peak profile in the PMMA target. GATE simulations of the setup utilized at KVI are also ongoing in order to compare the simulated and measured data.

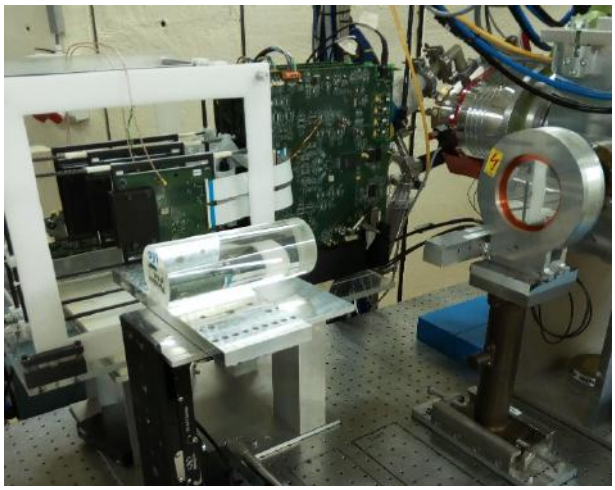

Fig. 8: Beam tests of MACACO II with 150 MeV protons on a PMMA target at the accelerator facility KVI-CART in Groningen (Netherlands).

As mentioned before, the Compton telescope provides two types of events: 'doubles' (events made of two coincident detections in two different planes) and 'triples' (events made of three coincident detections in three different planes). The image reconstruction developments for the laboratory tests have been mostly addressed to the use of doubles in the Compton telescope. Currently, there are two main lines of development. The first one keeps using doubles and it is aimed at using them more efficiently. The second main line of development aims at applying an appropriate image reconstruction code to the triples data to obtain the image. To this end, the physical models have also been extended to the triples case so that this type of events are properly included.

Perspectives of remaining challenges:

In spite of the significant performance improvement achieved with the Compton telescope featuring new detectors, the energy and timing resolution of the system are not yet those required by the application. The goal has been set to an energy resolution of 4% FWHM at 511 keV and a timing resolution below 1 ns FWHM. Alternative instrumentation is being tested in order to achieve such parameters. A two-plane Compton telescope is being mounted with a different readout system (PETsys2), which is expected to provide much improved timing resolution, while the energy resolution still needs to be assessed. Detectors employing SiPM arrays from a different manufacturer will be assembled and tested, expecting to achieve the energy resolution required.

On the image reconstruction side, at the moment double and triple event classes are used independently, *i.e.* two independent images of the same source distribution are obtained. In the future, the simultaneous handling of both types of events must be implemented during the image reconstruction process.

In addition, since the Compton telescope will work in high-background scenarios, where a reduced number of valid events is expected [Ortega 2015], background reduction strategies are a priority, both at the instrumentation level and in selection algorithms. Moreover, the enhancement of the image reconstruction algorithms to deal with low statistics scenarios is also foreseen as a challenge for the future.

Institut de Physique Nucleaire (IPNL), Lyon, France: (E. Testa et al.)

The PRISME group of the IPNL (Nuclear Physics Institute of Lyon) is involved in the medical physics research field, in particular in the development of gamma cameras for hadron therapy verification and nuclear medicine.
Hadron therapy is an emerging technique of cancer treatments using ion beams. The main therapeutic indications of this technique are the treatments of radio resistant tumors located near organs at risk and tumor treatments for children. Indeed hadron therapy allows the treatment of cancerous tumors whilst better sparing healthy tissues with respect to conventional radiotherapy using photons. In order to better benefit from the advantages of this technique, several studies are currently carried out worldwide to develop ion-range verification systems and hence to ensure that the treatment delivery is in accordance with the treatment planning. The detection of prompt gamma rays (PG) emitted during nuclear reactions undergone by some incident ions is one of the main techniques under study. The distribution of PG emission points is indeed strongly correlated to ion ranges.
On the other side, nuclear medicine consists in injecting radioactive substances into the patient for diagnosis and treatment of diseases. In the case of diagnosis, two types of modalities can be distinguished:
- Single Photon Emission Tomography (SPECT) that builds on detecting a given gamma line emitted from the radioactive substance with Anger cameras relying on physical collimation.
- Positron Emission Tomography (PET) that detects the 2 gammas resulting from the annihilation of positrons emitted by the radioactive substance. The detection of these two gammas in coincidence can be seen as an electronic collimation (no physical collimation) that allows in general for a larger detection efficiency.
In order to increase the detection efficiency in SPECT, the application of Compton cameras to nuclear medicine has been studied worldwide for several years. Originally designed for astrophysics applications, such cameras intend to perform an electronic collimation by maximizing the probability of Compton scattering in the first detector (scatterer) and the full gamma absorption in the second detector (absorber). The positions and energies deposited during these interactions determine a “Compton cone” as the location of the incident gamma direction. The distribution of gamma the source can then be reconstructed with image reconstruction algorithms that aim at determining the intersection of the various Compton cones.

Developments of Collimated and Compton cameras coupled to beam hodoscope (TOF gamma cameras):
The CLaRyS collaboration involving four French laboratories (IPN Lyon, LPSC Grenoble, CPP Marseille and CREATIS Lyon) develops two types of gamma cameras: a collimated camera and a Compton camera [Krimmer 2015] (Fig. 9).

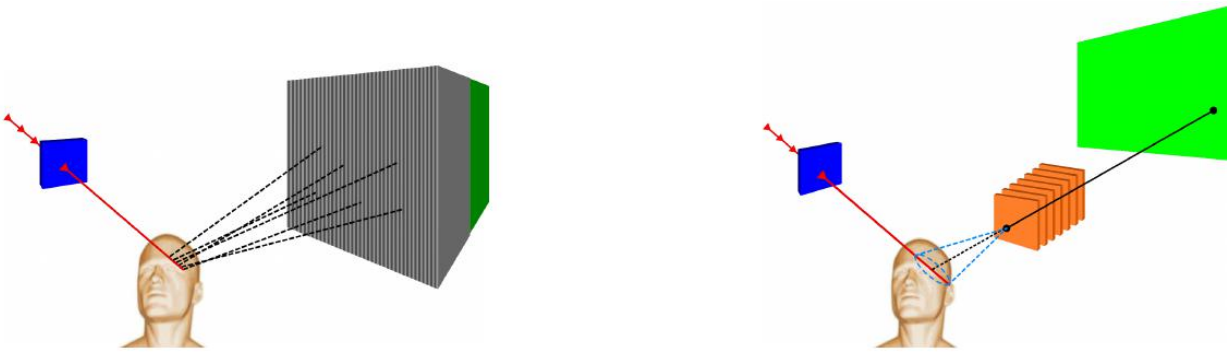

Fig. 9: Collimated camera (left) and Compton camera (right) coupled to a beam hodoscope developed for ion-range verification during hadron therapy. The hodoscope provides a measurement of the incident ion trajectory, while gamma detection by the collimated and Compton cameras corresponds to a plane and a Compton cone, respectively. The combination of the two types of information gives, respectively, one and two points among which lies the gamma emission point.

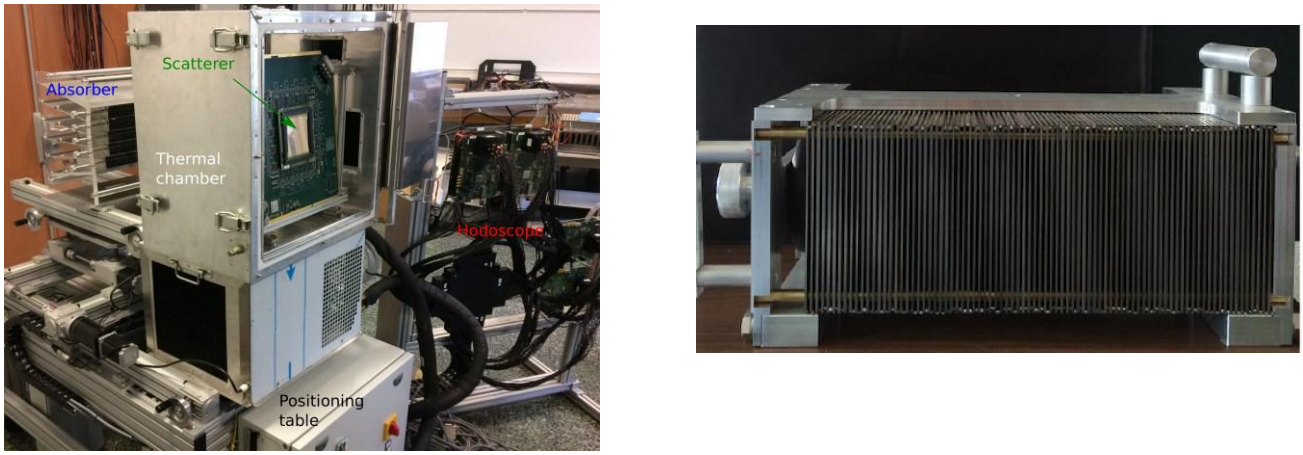

Fig. 10: Left: Picture of the "time-of-flight" Compton camera consisting of an absorber (scintillators, BGO blocks), a scatterer (semi-conductor detectors, 7 double sided silicon strip detectors located in a thermal box) and a scintillating fiber hodoscope . The camera can be converted into a collimated camera by replacing the scatterer with a tungsten alloy collimator (right).

A beam hodoscope with scintillating fibers is coupled to the gamma cameras in order to provide a spatial and temporal stamp of incident ions. This stamp allows for a first time-of-flight (TOF) selection of the particles detected in the gamma camera. Indeed, nuclear reactions lead to the emission of many neutrons that generate a large background. The TOF measurement allows for background reduction by selecting events in a TOF window centered on the PG arrival time. Moreover, the spatial stamp provides very good information on the PG emission point, which is likely to lie in the vicinity of the incident ion trajectory. The hodoscope under development consists of two planes of 128 scintillating square fibers of 1 mm^2 and a length of 140 mm.

The Compton camera consists of two detection sections (Fig. 10 left): a scatterer, composed of 7 planes of semiconductor detectors (double sided silicon strip detectors, 10x10 cm^2, 2 mm thickness) placed in a thermally regulated box and an absorber, composed of scintillators (BGO blocks 3.5x3.8 cm^2, 3 cm thickness). The Compton camera can easily be converted into a collimated camera by replacing the scatterer with a tungsten alloy collimator (Fig. 10 right). In order to cope with high counting rates expected in both hadron therapy and nuclear medi-

cine fields, the data acquisition system of the gamma cameras (coupled to the beam hodoscope) is based on the µTCA standard; originally conceived as an adaptation of the Advanced Telecommunications Computing Architecture (ATCA) systems used in the telecommunication field for high-flux data transfers, it has been adopted in the particle physics domain for about ten years [Abellan 2013]. In practice it allows us to deal with data rates up to 1 Gbit/s. During the last years, the absorber of the gamma cameras (Compton and collimated cameras) and the hodoscope have been partially characterized with laboratory and in-beam tests, in terms of spatial, energy and time responses. The three main results are the following:
- Characterization of the 30 BGO blocks of the absorber with an energy resolution of 23% at 511 keV and a time resolution of 4 ns FWHM (Full Width at Half Maximum) in accordance with the specifications [Fontana 2018].
- First in-beam test of the beam hodoscope with its final data acquisition system (Fig. 10, left) in the proton therapy center of Nice, France. The acquisition chain is operational although some optimizations are mandatory.

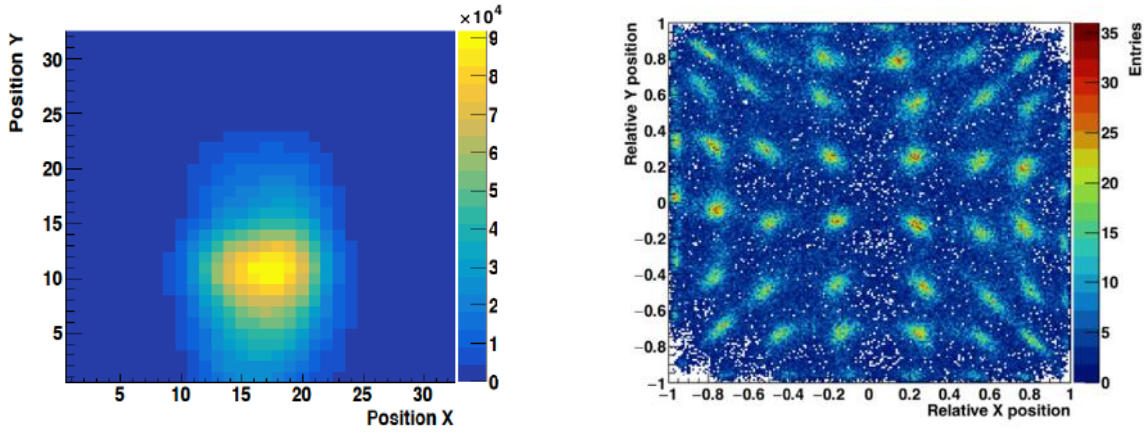

Fig. 11: Beam image obtained with the scintillating fiber hodoscope (left) and BGO block response with PG emitted from a plastic target irradiated with the 60 MeV proton beam in the protontherapy center of Nice, France (right)

- First in-beam test of the BGO blocks with PG emitted from a plastic target irradiated with the 63 MeV proton beam of the proton therapy center of Nice. We can see in the right panel of Fig. 11 the pseudo-pixel structure of the BGO blocks providing the spatial information (pixel width of 4 mm).
Extensive tests of these detectors are planned until mid-2019 as well as the characterization of the Compton camera scatterer. The first in-beam tests of the TOF- collimated cameras and Compton cameras are planned for mid-2019 and mid-2020, respectively.

Assessment of Compton camera performance in SPECT and hadron therapy verification
Developments in nuclear medicine generally make an extensive use of numerical calculations and more specifically of Monte Carlo simulations. Such simulations allowed us to assess the Compton camera performances both in the fields of SPECT and hadron therapy verification :

- SPECT: the Compton camera prototype of the CLaRyS collaboration has a detection efficiency 20 times as large as the one of an Anger camera of the same size. Besides its spatial resolution is slightly better above ~500 keV [Fontana 2017, Fontana 2017a]

- Hadron therapy verification: the signal-to-background ratio is poor at clinical intensities both with proton and carbon ion beams due to the high random coincidence rates. Reduced beam intensities are therefore mandatory

to perform ion-beam range verification, for instance during a few beam spots used as treatment probe before the full treatment.
GATE is an advanced open source software developed by the international OpenGATE collaboration and dedicated to numerical simulations in medical imaging and radiotherapy. It allows for complex Monte Carlo simulations (based on the Geant4 toolkit) using an easy-to-learn macro mechanism. A Compton camera module is currently under development in GATE within the CLaRyS collaboration and it has been validated against experimental data from the Compton camera developed in Valencia (MACACO prototype) [Munoz 2017].

Investigation of the PGPI technique
Several modalities of PG detection are currently being investigated worldwide. Apart from the aforementioned imaging techniques (collimated and Compton cameras), three non-imaging techniques have been proposed to provide indirect ion-range verification with relatively simple devices: Prompt Gamma Spectroscopy (PGS), Prompt Gamma Timing (PGT) and Prompt Gamma Peak Integral (PGPI) [Krimmer 2018]. The latter has been developed within the CLaRyS collaboration and the first experimental proof of principle of this technique has been recently published [Dauvergne 2016, Krimmer 2017].
PGPI consists in placing several scintillators around the patient to detect PG with a TOF measurement to discriminate PG generated in the patient from the room background mainly induced in the beam line. With a 3-inch diameter detector placed at a distance of 50 cm from the beam axis and 10^8 incident protons, corresponding to large irradiation beam spots, deviations of a few per cent in the PG count rate can be detected. For the present configuration, this change in the count rate corresponds to a 3 mm change in the proton range in a plastic target. Furthermore, simulation studies show that a combination of the signals from multiple detectors may be used to detect a misplacement of the target. A different combination of these signals provides an information on the deposited energy in the patient, which is independent from the actual target position.
Further studies with Monte Carlo simulations are planned in 2019 to investigate the potential of the technique in more realistic conditions.

LPSC Grenoble (France): (D. Dauvergne et al.)

The LPSC team Nuclear Physics and Medical Applications is working on detection techniques for the online control of innovative radiation therapies, in collaboration with biologists, radiotherapists and medical physicists:

• with photon radiations (X-ray radiotherapy), with Intensity Modulated Radiotherapy, and synchrotron radiation therapy, for which either a strong enhancement is obtained by means of heavy atoms selectively added in the tumor, or using strong spatial fractionation (at the micrometric scale), making it possible to improve the differential effect between tumor and healthy tissue,
• with proton or light ion beams (hadron therapy), for which the ballistic precision and the efficiency of the dose deposition are optimized by a maximum dose deposition at the end of the ion path in the material.

The emergence of these radiotherapy modalities, or the improvement of efficiency for existing techniques, requires the development of instrumentation for the control of treatments both for photons and particle beams. The detector system developed under the name of TraDeRa is a typical example of a detector developed at LPSC Grenoble in collaboration with the University Hospital of Grenoble. This detector is aimed at operating such a treatment control in real time during Intensity Modulated Radiotherapy. In Intensity Modulated Radiotherapy, the photon beam is produced by a linear electron accelerator. It is dynamically shaped by collimation slits to optimize the dose deposition in the tumor. TraDeRa is a near-transparent x-ray detector. It is located upstream of the patient and is positioned on the accelerator head. It is a pixelated detector, allowing for the measurement of

the characteristics of the irradiation beam in two dimensions. Dedicated readout electronics has been realized entirely at the LPSC: on-board charge integration allows a reading of the flow of photons in real time.

The first prototype, shown in Fig. 12, allows the monitoring of an irradiation field up to of 25 cm x 25 cm, with 340 readout channels. It has been tested at University Hospital and it is able to detect mispositioning on a single collimation blade as low as 1mm. A second prototype with 1600 signal readout channels, with a field of view of 40 cm, was assembled and tested. This prototype makes it possible in particular to perform wireless data transfer, which makes the system easily portable in clinical conditions. The integrated electronics (ASIC circuit) allows the integration of charge with sufficient dynamics for a response of the detector at the millisecond scale [GallinMartel 2016].

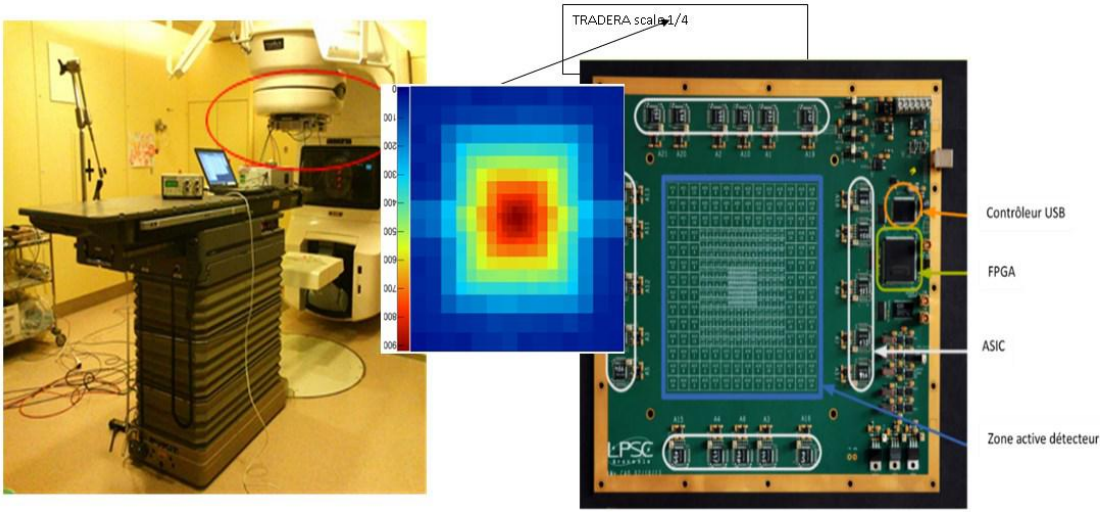

Fig. 12: ¼-scale demonstrator positioned at the hospital LINAC head in Grenoble. Right: detector board

An important simulation work [Fabbro 2017] was conducted to model the photon flux coming from an accelerator head, and thus to allow in the long term to predict the response of the detector according to the parameters of the accelerator, and to translate the 2D response map of the studied X field into a 3D dose in a water tank used for quality control. TraDeRa is a tool in the quality assurance chain of adaptive radiotherapy, which has been patented and for which a valorization action is in progress.

Diamond hodoscope:

Diamond detectors, thanks to their structural and electronic properties, are ultra-fast detectors with a resolution in time of the order of a few tens of picoseconds, with a low background noise, and resistant to radiation. As part of the CLaRyS French national collaboration, our project is focused on the design of a beam hodoscope, which will be integrated into a secondary prompt radiation detection system, to control ion range in hadrontherapy. Indeed, such radiations, induced by the nuclear collisions, are emitted throughout the path of the ions (by a small fraction of them), which makes it possible to measure their range. Such an on-line control device will improve the ballistic accuracy of hadron therapy treatments by reducing the uncertainty margins associated with treatment planning, morphologic changes, patient positioning and motion.

The goal here is to develop large area detectors with a high detection efficiency for carbon or proton beams providing time and position measurement at 100 MHz count rates (beam tagging hodoscope). Commercial Chemical Vapor Deposited (CVD) poly-crystalline, hetero-epitaxial and monocrystalline diamonds were studied in view of a future assembly. Plasma microwave aluminum metallization is performed in order to make conductive contacting surfaces. The applicability of these diamonds as particle detector was investigated using α and β radioac-

tive sources, 95 MeV/u carbon beams (see Fig. 13) and short-bunched 8.5 keV photons from the European Synchrotron Radiation Facility (ESRF). A time resolution ranging from 20 ps up to 40 ps rms and an energy resolution ranging from 7 % up to 10% were measured, depending on the energy loss rate, and thus on the irradiation species [Collot 2017, GallinMartel 2018].

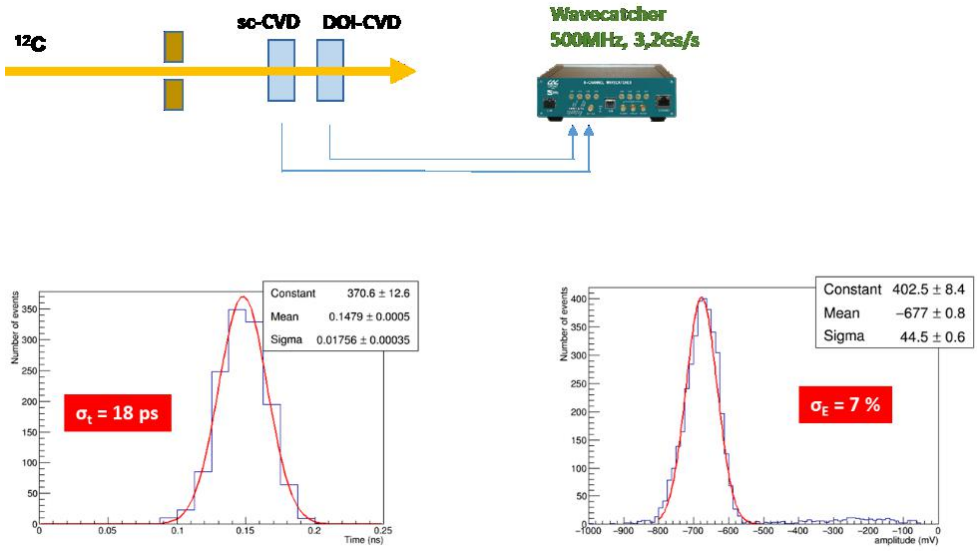

Fig. 13: Scheme (top) and results of an experiment with a 95 MeV/u carbon ion beam impinging on two successive diamond detectors. A fast waveform digitizer (Wavecatcher) is used to record pulses and analyze the time resolution between two detectors (bottom left) and their energy resolution (bottom right, for the single crystal).

These tests enabled us to conclude that polycrystalline CVD diamond detectors are good candidates for our beam tagging hodoscope development. The final detector will consist in a mosaic arrangement of double-sided stripped diamond sensors read by a dedicated integrated fast read-out electronics (~1800 channels). First assemblies of double-side stripped detectors, with discrete electronics readout, have been mounted and tested, as illustrated in Fig. 14 with a 1 cm^2 polycrystalline diamond plate.

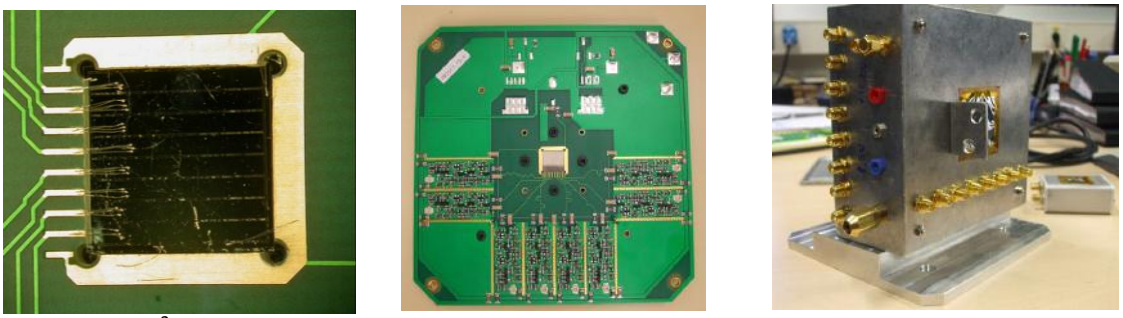

Fig. 14 : 1 cm^2 double-sided diamond strip detector. Left: zoom on the stripped and bonded detector mounted on PCB support, center: detector board with current preamplifiers, right: detector box with connectors.

Future challenges and perspectives:

The TraDeRa prototype is currently under evaluation. Eventually, a prototype integrating a software suite of characterization of the irradiation defects will be produced, and delivered to the equipment manufacturers in the field

of radiotherapy quality control. The creation of a spinoff company is under consideration. Besides, new developments are undergoing for very high photon flux monitoring.
A new challenge is opened with the forthcoming clinical trials at the European Synchrotron Light Source (ESRF) beamline ID17, using microbeam radiation therapy. Indeed, the beam is spatially fractionated with above 1000 Gy/s delivered in narrow peaks of a few tens of µm, separated by 300-500 µm. Online control of such dose delivery requires fast and high-dynamics detection devices, for which the Grenoble team will conjugate their knowledge in multi-channel charge integration electronics, and large area segmented diamond detectors. A PhD student started on this topic.
As for fast timing for secondary radiation detection in particle therapy, it is now being investigated, experimentally and with simulations, the benefits of 100 ps timing resolution in prompt-gamma control of proton therapy. Indeed, ultra-fast gamma detection may replace collimated devices, and thus enhance the detection efficiency for real-time control. Such a device will couple a diamond hodoscope and fast scintillators.

OncoRay (Dresden, Germany): (G. Pausch et al.)

The In-vivo Dosimetry group at OncoRay in Dresden (Germany) has intensely dealt with the problem of in-vivo range verification in proton therapy. The latter has become a widely accepted and promising option for tumor treatments complementing conventional radiotherapy. The finite range of protons in tissue with a final dose maximum (Bragg peak) followed by a sharp distal dose fall-off allows focusing the dose in the tumor, while minimizing the damage of surrounding normal tissue. The proton range is, however, sensitive to factors that are hard to assess in clinical routine. This constrains the potential benefit of a proton treatment over conventional therapies performed with megavolt X-rays and electrons. Reducing proton range uncertainties would improve the precision and lower the normal-tissue toxicity of proton therapy. Therefore research groups all over the world have tried to develop clinically applicable instruments for measuring the proton range just during dose delivery, ideally with a precision of one or two millimeters. Prompt gamma rays are generally considered the most appropriate probe. This hard radiation is produced in nuclear reactions by beam particles hitting atomic nuclei of the penetrated tissue.
In this context, OncoRay has dealt with nuclear instrumentation for in-vivo range verification and other medical applications.

Detector development for PGT
OncoRay invented the Prompt Gamma-Ray Timing method (PGT) for proton range verification in tumor treatments [Golnik 2014]. PGT analyzes the time distribution of prompt gamma rays, detected by fast scintillation detectors, relative to a signal referencing the delivery of proton micro-bunches, actually the accelerator radiofrequency (RF) tapped from the therapy facility. The width of the time distribution reflects the finite stopping time of the protons in tissue, which depends on their range.
Clinically applicable hardware in the form of PGT detection units was developed in order to translate this technique to the clinics. It consists of bright $CeBr_3$ scintillators, read out with classical photomultiplier tubes (PMT), which are coupled to ultrafast, high-resolution timing and energy spectrometers [Pausch 2016]. This hardware provides excellent gamma-ray spectroscopy properties with an energy resolution of 1.2% at 6.1 MeV as well as a time resolution around 250 ps in the energy range of prompt gamma rays [Pausch 2018] Tests under clinical beam conditions have meanwhile proven the PGT principle and yielded encouraging results at clinical beam currents [Werner 2017, Werner 2018]. The hardware is also well suited for other applications where excellent spectroscopy has to be combined with robustness and compactness.

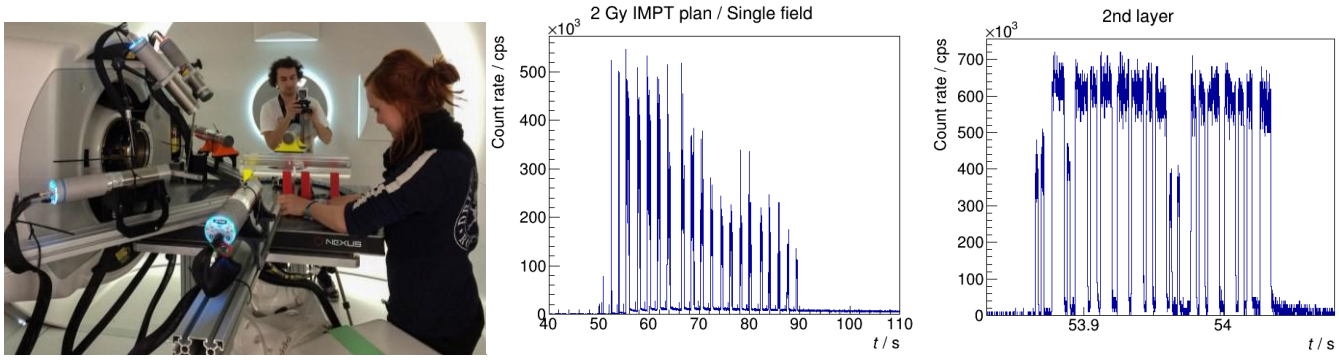

Fig. 15*:* The photograph (left) shows six PGT detection units in an experiment performed in the treatment room of the University Proton Therapy Dresden (UPTD). Exemplary count rate histograms disclose the time structure of PBS treatments. During beam delivery, the count rate jumps up to 700 kcps due to the detection of prompt gamma rays. In beam breaks, the count rate is only due to target activation. Energy layers and single PBS spots are clearly separated in the plots shown in the middle and right panels, respectively [Pausch 2018].

Gain and timing stability of PGT detectors at high load and strong load leaps

Clinical treatments with proton beams are distinguished by harsh conditions differing very much from those at research accelerators [Pausch 2018]. The treatment is usually performed in pencil beam scanning (PBS) mode, the most advanced, economic, and gentle technique of dose delivery in recent clinical facilities. The tumor is scanned in three dimensions with a beam focused to about the diameter of a pencil. A PBS treatment plan is organized in so-called energy layers, corresponding to different irradiation depths, each layer comprising a finite number of distinguished spots of the same beam energy, but different lateral positions. Spots and layers are separated by beam breaks. This means enormous leaps in the production of prompt gamma rays as well as in the detector load, as shown in Fig. 15 (middle and right panel). The stability of the detectors' gain and timing properties under such conditions had to be explored. Selected results were published recently [Pausch 2018a], some are given in Fig. 16. As a consequence, dedicated correction procedures for detector gain and timing had to be developed. They must be applied when analyzing PGT data sets taken during experiments or treatments [Werner 2018]. With these corrections, the energy and time resolution of the PGT hardware can be kept for detector loads up to 1-2 Mcps even if load and system throughput change at a time scale of milliseconds to seconds (Fig. 16).

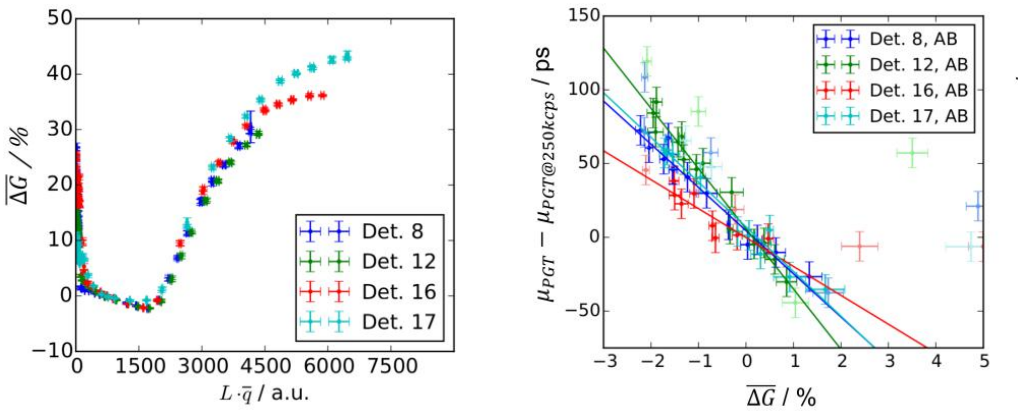

Fig. 16: Relative gain drift as a function of the mean PMT anode current, represented as the product of detector load and mean charge per detector pulse (left panel), and correlation between relative gain drift and timing shift (right panel) [Pausch 2018a]. The latter allows correcting for timing shifts by monitoring the detector gain.

Single-plane Compton imaging

A third topic pursued is a novel imaging technology named single-plane Compton imaging (SPCI) [Pausch 2016, Koegler 2018]. SPCI builds on pixelated scintillation detectors with individual pixel readouts, similar to those developed for combined positron emission tomography – magnetic resonance imaging (PET-MRI) systems, where each scintillator pixel is coupled to a single silicon-based photosensor. Information about the incident angles of gamma rays is here derived from the energy sharing between two (adjacent) detector pixels in case of events distinguished by a Compton scattering process in the first pixel followed by full absorption of the scattered gamma ray in the second pixel. Corresponding experiments have been performed with a 4x4 GAGG scintillator array coupled to an array of digital silicon photomultipliers (dSiPM), as sketched in Fig. 17, exposed to 662 keV gamma rays from a ^{137}Cs point source. The effect of the source position on the energy sharing is demonstrated in Fig. 17 for an exemplary pixel pair. Image reconstruction with a basic maximum likelihood expectation maximization (MLEM) algorithm, using a set of base functions (energy sharing distributions for all possible pixel pairs) measured for a 2-dimensional image space, could indeed reproduce the position of a single as well as for multiple point sources [Koegler 2018].

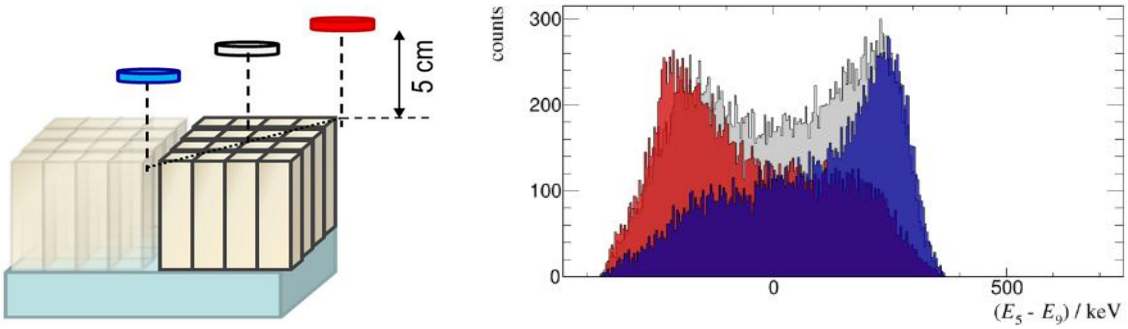

Fig. 17: Sketch of the experimental setup for proving the SPCI principle (left panel) and exemplary energy sharing distributions (right panel) for the three source positions marked in the sketch [Koegler 2018]. The distributions exhibit the difference of energy depositions in pixels 5 and 9 for those coincident events distinguished by a sum energy of 662 keV, indicating full absorption of the initial gamma ray in two steps (Compton scattering of the initial gamma ray in one pixel followed by photo-absorption of the scattered gamma ray in the other pixel).

This first experimental proof of principle encourages further investigations. Applications for imaging in nuclear medicine [Pausch 2016], but also for proton range verification [Pausch 2018] are envisaged.

University "La Sapienza", Rome/Italy: (V. Patera et al.)

The Italian particle therapy community is addressing the burning need to reduce the presently large safety margins (up to 10 mm around the tumor) applied in particle therapy treatment plans, as they prevent *de facto* a full exploitation of the therapeutic potential.

The INSIDE system (INnovativeSolutIons for Dosimetry in HadronthErapy) is an innovative bimodal imaging system providing a robust method of ion range verification during particle therapy treatments [Marafini 2015, Bisogni 2017]. The physical principle underpinning the INSIDE operation is the nuclear fragmentation of the target and of the projectiles (for carbon ions) that produces *beta*$^+$ radioactive nuclei and secondary charged radiation (mainly protons) along the beam path. Detecting such fragmentation products provides an insight of the ion range. INSIDE stems from a collaboration between the University of Pisa, the University of Rome "Sapienza", the University of Turin, Politecnico of Bari and the National Institute of Nuclear Physics (INFN) and, for the clinical trial, the National Center for Oncological Hadrontherapy (CNAO). The ultimate goal of the project is the development of an auto-

matic procedure to control the particle range based on the comparison between data acquired during treatments and simulated from treatment plans, in order to highlight in real time any discrepancies with respect to the expected plan.

The INSIDE bimodal system consists of a positron emission tomography (PET) scanner for annihilation radiation detection and of a dose profiler (DP) for secondary charged particle tracking. The two detectors are supported by a mobile structure designed to easily position and remove INSIDE at the CNAO treatment site such as to minimize the impact on the clinical protocol [6-Bisogni 2017].

Charged secondary particles are particularly suitable to monitor the beam range in Particle Therapy with carbon or oxygen ions. The secondary charged fragments produced in the interaction between the beam and the patient tissue escape the patient and can be detected with very high efficiency in a nearly background-free environment. Recent experiments demonstrated that the longitudinal emission distribution of such fragments is related to the beam range inside a human tissue-equivalent target [Piersanti 2014].

Charged secondary fragments are preferentially forward emitted but a non-negligible fraction of secondary protons produced by ^{12}C ion beams are emitted at large angles (ϑ=60°–90°) as well [Piersanti 2014]. The production of secondary protons at large angles is particularly interesting due to geometrical consideration: the beam transverse profile worsens the spatial resolution of particles reconstructed trajectories by a factor proportional to $(\sin\vartheta)^{-1}$. Moreover, going to large angles simplifies the positioning of the range detector in a treatment room with respect to the patient.

There are two main shortcomings for a beam range monitor based on charged secondary particles: 1) the charged secondaries suffer multiple scattering when crossing the patient and 2) need a minimum kinetic energy to exit the patient's body. Therefore, a limited fraction of the produced particles is available for monitoring purposes. Such factors limit the spatial resolution that can be achieved when reconstructing the Bragg peak (BP) position, i.e., the beam range. To collect sufficient statistics of charged secondary particles, the angular acceptance of the detector needs to be increased in order to achieve the needed resolution on the BP position.

Such a beam monitor technique has been exploited within the RDH/INSIDE project: the dose profiler (DP) [Traini 2017], a charged secondary particle tracker based on scintillating fibers has been designed and built to be used as range monitor for the CNAO carbon ion beam.

DOSE PROFILER LAYOUT

The DP is composed by eight planes of two orthogonally placed scintillating fiber layers, each made of 384 fibers of 500 × 500 μm^2 squared section (multi-cladding BCF-12 from Saint-Gobain), in order to reconstruct the 3-D coordinates of the proton track. Fibers composing a layer are glued together. The minimal separation of 2 cm between two consecutive planes is a tradeoff between the need to increase the tracker spatial resolution and the detector compactness, needed for the space limitations in a treatment room, and large geometrical acceptance, which increases the reconstruction efficiency. The choice of the fiber size is the result of an optimization aiming to balance signal amplitude and the total amount of material to be crossed by charged particles. The total size of the detector is 28 × 28 × 31 cm^3. Fig. 18 shows the DP layout and the principle of secondary proton reconstruction.

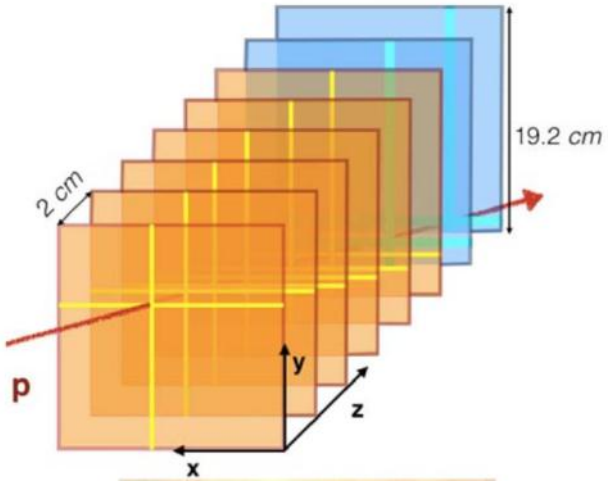

Fig. 18: Scheme of the Dose Profiler detector and the related detection principle for a proton. The orange detector planes are positioned near the patient.

In order to optimize the charged particle detection, the choice of the angle at which the detector has to be placed with respect to the beam direction is crucial. At narrow angles, there is the advantage that the emission flux is enhanced. On the other hand, the detected emission shape is convoluted with the transverse beam spot size projected on the beam line; therefore, the spatial resolution on the emission shape worsens for angles different from 90°. As a compromise, in INSIDE, a detection angle of 60° has been chosen.
The fibers readout is performed by means of 1 mm^2 silicon photomultipliers (SiPMs). Since each fiber is 500 μm , each SiPM reads two adjacent fibers. In order to read the whole 384 fibers, SiPMs are alternately coupled to the fibers on both sides, so that a single layer is read by 192 channels. The SiPMs are readout by BASIC32_ADC [Ciciriello 2013], 32-channel Application Specific Integrated Circuits (ASICs) specifically developed to read out SiPM detectors in medical imaging applications. The BASIC32_ADC, 32-channel ASICs are configured and read-out by a set of field-programmable gate arrays. The system has been tested at the CNAO center in clinical conditions, and a maximum sustainable rate of ~100kHz has been measured. The detector provides an internal trigger system, optimized for proton tracks triggering.
The detector has been mounted in the treatment room of the CNAO center and will be tested during patient treatment in the first months of 2019.

The MONDO neutron tracker

The secondary neutron component produced during a particle therapy treatment is another issue to be tackled and carefully taken into account when planning the treatments to improve the accuracy and the quality assurance of particle therapy. Secondary fast and ultrafast neutrons are produced in nuclear interactions of proton and carbon ion beams with patient tissues (see Fig. 19) as well as charged secondary particles, with the energy of hundreds of MeV. They can deposit their energy far from their production point. This effect must be strictly taken under control in view of secondary-malignant neoplasms especially in pediatric patients who have a longer life expectation [Newhauser 2011].

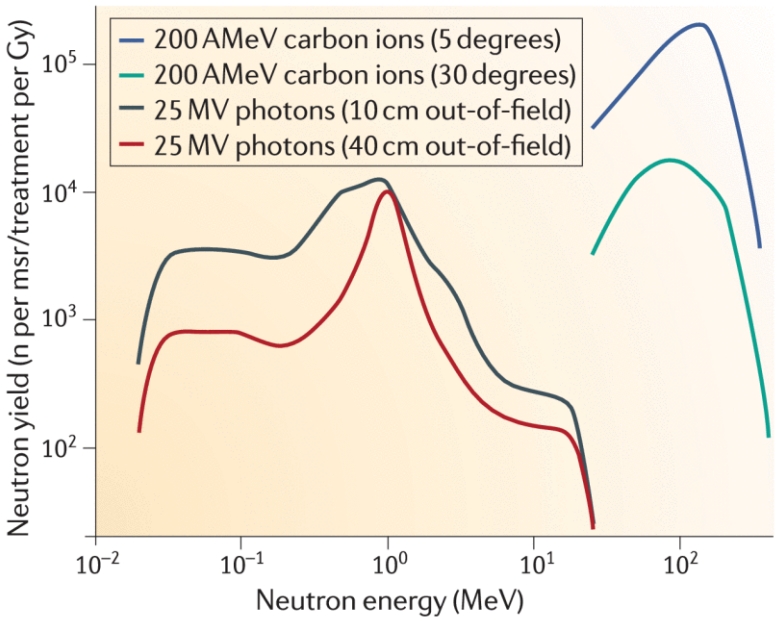

Fig. 19: Secondary neutron yield as a function of the energy of photo-neutrons produced by 25 MV X-rays and secondary neutrons produced by nuclear interactions of 220 MeV/u carbon ions with a water target. Photo-neutrons were measured at 10 cm (black) or 40 cm (red) from the target area. Secondary neutrons produced by ^{12}C ions were measured at 5° (blue) and 30° (red) with respect to the beam direction. These different spectra result in different (organ-specific) risk factors.

Nowadays, an accurate and complete characterization of secondary neutron energy spectra as a function of the emission angle is still missing: detectors capable of reconstructing the neutron direction at energies of interest in PT have not yet been developed. Therefore, the treatment planning system presently has not an accurate prediction capability of the effects induced by the neutron dose release. The aim of the Monitor for Neutron Dose for Hadrontherapy (MONDO) experiment [Marafini 2017] is to characterize the fast and ultrafast neutron radiation produced in PT treatments with the aims to optimize the treatment plan, and, possibly, to understand if a correlation exists between the neutron emission and the primary beam range for range monitoring purposes.
The MONDO detector is a secondary fast and ultrafast neutron tracker, using the scintillating fibers as an active medium to track secondary neutrons produced in nuclear interactions of PT heavy ion beam with patient tissues, reconstructing the neutron 4-momentum exploiting the double elastic scattering (DES) in the tracker interacting material (see Fig. 20).

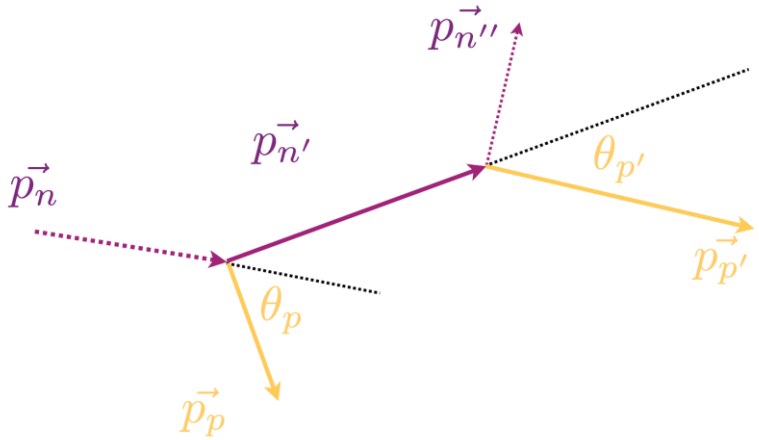

Fig. 20: Scheme of a Double Elastic Scattering reaction.

In a single elastic scattering interaction, a recoil proton is produced and the following equation describes the relationship between the neutron (*pn*) and proton (*pp*) momenta and the proton diffusion angle (ϑ_p).

$$p_n = \frac{p_p}{(cos\theta_p)^2}$$

If the diffused neutron (*n*') undergoes another elastic scattering interaction, and another recoiling proton (*p*') is produced, using the same relation, and knowing the diffused neutron direction (and therefore, the diffused *p*' angle $\vartheta p'$) connecting the two interaction vertexes, it is possible to reconstruct the primary neutron momentum and incoming direction.

In order to track neutrons and to measure their 4-momentum, the MONDO detector will, therefore, track the two recoiling protons from neutron DES reactions. To maximize the neutron DES interaction probability, the detector will be made of a highly hydrogenated material as an active medium. It will be composed by subsequent orthogonal layers of 250 ×250μm^2 squared plastic scintillating fibers that will contemporarily act as a target for neutrons and detector for recoil protons. A proton crossing layers of fibers will lose energy, producing scintillation photons that will be detected and allowing to reconstruct the proton direction. The proton energy will be measured from its range in the tracker material, asking for the full containment of the recoiling track. The small fiber size is, therefore, a tradeoff between the scintillation light that needs to be detected and the achievable spatial resolution on the reconstructed track. Three is the minimal number of crossed layers in both orthogonal views in order to reconstruct a proton track, corresponding to a total amount of plastic scintillating material of 1.5 mm and to a proton energy threshold of 12 MeV. The final detector size will be 10×10×20 cm^3, allowing to measure neutrons up to 400 MeV of energy.

INFN – University of Pisa (Italy): (M.-G. Bisogni et al.)

The second main component of the previously addressed INSIDE detector system, the PET detector, developed in collaboration between University and INFN Pisa and Turin, is made of two planar opposite heads, with 60 cm of distance from one to the other, each composed of 10 (array of 2x5) detection modules. A detection module is an array of 16x16 lutetium fine silicate (LSF) scintillating crystals, 3x3x 20mm^3 each, optically coupled to a matching array of silicon photomultipliers (SiPMs). The head total area of 112 mm (transaxial) x 264 mm (axial, along the beam direction). The DP, developed by the University and INFN Rome and Milan, is made of 8 scintillating fiber layers, that allow for reconstructing the track and to extrapolate the emission points of protons exiting the pa-

tient with about 90 % efficiency. The 19.2x19.2 cm^2 DP planes are made of square (500 x 500 μm^2) multicladding fibers read out by SiPMs [Muraro 2006].
The PET system was installed and has been in operation at CNAO since 2016. After the commissioning phase, it has been successfully used to monitor a patient with a lacrimal gland tumor in two consecutive treatment sessions.
In particular, the vertex field (treatment bed parallel to the beam direction) of the fractions 28 and 29 out of 30 was monitored. Both the irradiations lasted 240 sec [Ferrero 2018]. The patient was treated with 3.7 x 10^{10} protons per field (dose 2.2 GyE) in the range [66.3, 144.4] MeV/u. The acquisitions were also compared with Monte Carlo simulations reproducing the same set-up. Figure 13 shows the activation maps reconstructed after 240 sec of irradiation and additional 30 sec of acquisition after-treatment (left: experimental data collected on the first day; right: simulation; the beam enters from top) [Fiorina 2018].

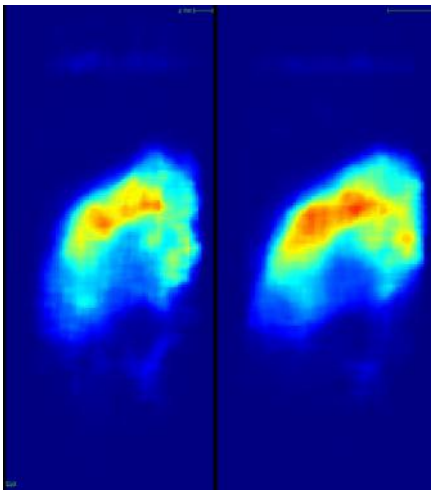

Fig. 21: Activation maps reconstructed after 240 sec of irradiation and additional 30 sec of acquisition after-treatment. Left: experimental data of the first day. Right: simulation. The beam enters from top. Color map legend: maximum intensity in red (a.u.), null intensity in blue.

The DP was completed and tested at CNAO with phantoms since the second half of 2017. Figure 19 shows the distribution of the secondary protons generation depths along the beam direction (red down-triangles) as obtained irradiating an anthropomorphic phantom with 300 MeV/u ^{12}C ion pencil beams. The distribution has been obtained with 10^6 ions integrated on 1 cm^2 area transversal to the beam direction. Taking into account the absorption of the secondary proton in the patient tissue by means of a filtering procedure (see [Traini 2017]), the emission profile (green up-triangles) was calculated. The simulated emission distribution (Monte Carlo truth) is also shown for comparison (black squares).
During the testing phase, the limits of the current mobile structure have emerged. The dimensions do not allow for a satisfactory integration in the nozzle and prevent the use of INSIDE in most of the treatments carried out at CNAO. Furthermore, the manual positioning of the trolley does not allow for achieving the best precision required for the measurement of the particle range. For these reasons, in 2018 a thorough revision of the mobile structure and of the positioning system at the nozzle was carried out to allow for the clinical validation of INSIDE. Fig. 20 shows the updated version of the INSIDE system as installed in a treatment room at CNAO. 20 patients for head and neck cancers will be soon enrolled for a clinical trial. Those patients will be monitored with the INSIDE system during their whole therapeutic cycle for longitudinal studies on the treatment efficacy.

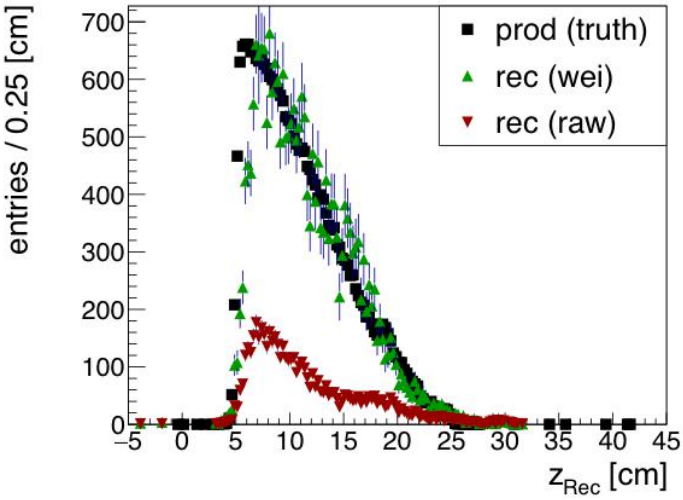

Fig. 22: Distribution of the secondary protons exiting an anthropomorphic phantom. Emission profile after absorption correction (green up-triangles). The simulated emission distribution (Monte Carlo truth) is also shown for comparison (black squares).

Fig. 23: Picture of the updated version of the INSIDE bi-modal system. The PET heads are visible above and below the treatment bed. The DP is on the upper left side, pointing toward the isocenter.

LIP/ University of Coimbra, Portugal: (P. Crespo et al.)

Proton beam range monitoring instrumentation is being developed by the team in Coimbra in the framework of the so-called orthogonal prompt gamma imaging (O-PGI) technique, where simulations [Biegun 2012, CambraiaLopes 2018] and single-slit, phantom-based experimental results [CambraiaLopes 2015] have shown to hold promise in improving proton therapy. A full O-PGI system is applied by interfacing a multi-parallel-slit collimator between the patient and a flat-panel-type gamma-ray detection system [CambraiaLopes 2017]. This detection system must be electronically time-correlated with the radiofrequency (RF) of the proton cyclotron in order to reject neutron-induced secondary gamma rays that highly disturb O-PGI. Such a rejection is based on the so-called

shifting-time-of-flight (shifting-TOF) method [Biegun 2012, CambraiaLopes 2018], i.e. a TOF-based mechanism that takes into account the time necessary to stop the incoming proton in the patient. Realistic patient-alteration scenarios have been studied by simulations, yielding an optimal collimation system [CambraiaLopes 2018]. However, gamma-ray detection granularity has not yet to date been explored, nor the optimum positioning of such gamma-ray detectors. These are part of the first goals of an ongoing project. In addition to gamma-ray granularity and positioning, the type of scintillator and scintillation readout detectors must also be optimized via simulations. E.g., fast scintillator materials and corresponding scintillation detectors must be chosen in order to sustain the high repetition rate delivered in therapeutic proton beams, together with the capability to provide enough shifting-TOF rejection. In addition, radiofrequency (RF) occupancy scenarios must also be investigated in order to find a proper detector readout that does not compromise the premises obtained by simulation (e.g. pulsed readout with shifting-TOF applied on an event-by-event basis, together with a low-energy threshold, or integration readout applied on an RF-period basis together with shifting-TOF rejection). Finally on this topic, radiation hardness must also be studied by simulations and by means of in-beam experiments such that the proposed detectors endure several (tens of) years of operation under harsh therapeutic conditions. In parallel to these goals, other foci of the ongoing project consist of designing and building a smaller-scale O-PGI prototype (i.e. multi-slit and multi-channel) and testing it on a proton-therapy beam in conditions that allow for confirming or rejecting the assumptions made in the simulations. For that, imaging with beam currents lower than therapeutic ones (~$3x10^{10}$ protons/s) must first be performed, together with a high beam energy of ~200 MeV, and patient-like phantoms irradiated on the treatment couch. In addition to simulation validation, the output of such prototype testing will serve as input for a final specification of a full O-PGI system to be constructed either at a laboratory level (e.g. LIP), or in close collaboration with industry (a multitude of private companies design detectors and data acquisition systems for gamma-ray imaging, not to mention clinical proton cyclotron manufacturers themselves). It is also the objective of the present exploratory project to focus on the problems inherent to target (tumor) motion, mainly due to the respiratory cycle, which currently limits applying narrower margins in, e.g., lung tumor irradiation. With this purpose, simulations with a digital anthropomorphic phantom will be carried out in order to explore the possibility of using O-PGI to track in real time such irradiation conditions, hence opening the door to restrictions of the dose volume in lung irradiation. Finally, total body irradiation (TBI) with proton therapy in pediatric patients is also challenging, due to the positioning of the vertebra in a spinal cord that is known to may have suffered from elongation and/or contraction on a day-to-day basis. The last purpose within this project is to derive by simulation and experiment (with proper anthropomorphic phantoms) the degree of confidence that O-PGI would provide to monitor TBI in pediatric patients.

Status and perspectives for instrumentation for medicine:

Due to the precision limitations of proton therapy stated several times before, an imaging system capable of detecting in real time whether the Bragg peak is being deposited in the predicted location is being investigated worldwide, both by research institutions/universities and by proton cyclotron manufacturers themselves in collaboration with the aforementioned research institutions. One of such real-time-capable imaging system is the orthogonal, multi-slit prompt-gamma imaging (O-PGI) system presently being evaluated.

In the following the potential advantages for monitoring in real-time simulated clinical scenarios of pertinence, such as an irradiation in the region of the pituitary gland with and without the formation of cerebral edema or scar tissue [Denham 2002] are put forward. It must be stated that these results are conservatively termed “potential” even if some experiments have already been carried out, although only with a homogeneous phantom and reduced beam current [CambraiaLopes 2015, CambraiaLopes 2017, CambraiaLopes 2011].

Simulated time spectra of photons and neutrons after passing through the multi-slit collimator, for proton irradiations of the anthropomorphic phantom in the pelvis (worst-case scenario) are shown

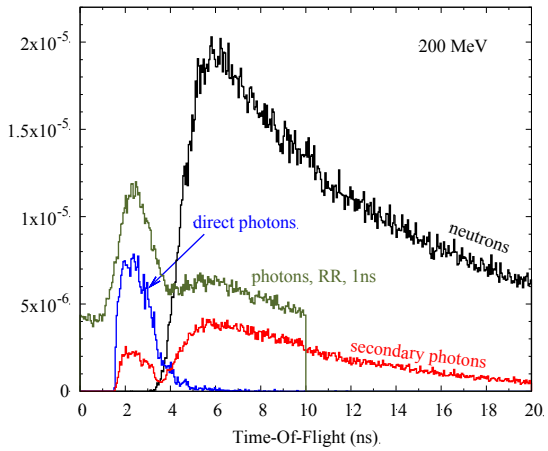

Fig. 24: Simulated time spectra of photons and neutrons after passing through the multi-slit collimator, for proton irradiation of the pelvis (worst-case scenario). Time-of-flight values are defined as the time difference between the creation of the proton and the arrival of a particle at the detector. Photons were assigned as 'secondary' if they interacted and/or were created in the collimator; otherwise, photons were assigned as 'direct'. The curves labeled 'RR, 1ns' represent all direct and secondary gammas arriving at the detector subject to a realistic cyclotron repetition rate of 100 MHz and a proton bunch width of 1 ns FWHM.

in Fig. 24 only direct photons contribute to a useful image, being correlated with the incoming proton beam. Secondary photons disturb the imaging conditions by introducing a blur in the image. As it can be seen, the counts of secondary photons arriving at the same time as that of direct photons are one order of magnitude below with respect to the counts of direct photons, meaning they will not disturb O-PGI. However, secondary photons produced by neutron-induced reactions in the collimator are almost as numerous as the counts of direct photons (green curves in Fig. 24). These can be rejected by applying a shifting time-of-flight window (shifting TOF) to the incoming data, as explained in [1-Biegun 2012, 2-CambraiaLopes 2018] and proven by experiment in [CambraiaLopes 2015]. The term "shifting" applies due to the fact that detectors that are positioned more to the left will see the direct photons arriving first with respect to detectors positioned more to the right. This is due to the stopping time of the protons in the target, which can lead to time deviations as large as 2 to 3 ns [CambraiaLopes 2018].

Detecting a 2-mm shift in Bragg peak location within an anthropomorphic phantom:

Fig. 25, left (taken from [CambraiaLopes 2018, CambraiaLopes 2017]), shows a simulation with an anthropomorphic phantom, where a clinically-realistic proton beam is shot in the head, in the region of the pituitary gland. Repeated irradiations may lead to injuries in the vascularity of the tissues (conjecture 1), thus resulting in increased permeability and, hence, the formation of edema in the tissues crossed by the beam. Being that the brain density is approximately 1.040 g/cm^3, and water has a density of about 1.000 g/cm^3, the aforementioned situation (deviation of only 4% in brain density) results in an over-range of the Bragg peak of 2 mm, as shown in the image. The tumor location will be under-dosed. On the other hand, formation of scar tissue may also occur [Denham 2002] (conjecture 2), which may lead to increased density of the tissue. By assuming this density change to be also about 4%, one obtains a Bragg peak under-range of approximately 2 mm (same image). In Fig. 25, right, it can be seen that the aforementioned deviations of the Bragg peak can be detected with an O-PGI system. Furthermore, the right image in Fig. 25 shows that an automatic linear regression fit applied to the data can reveal such deviations with no need for human intervention.

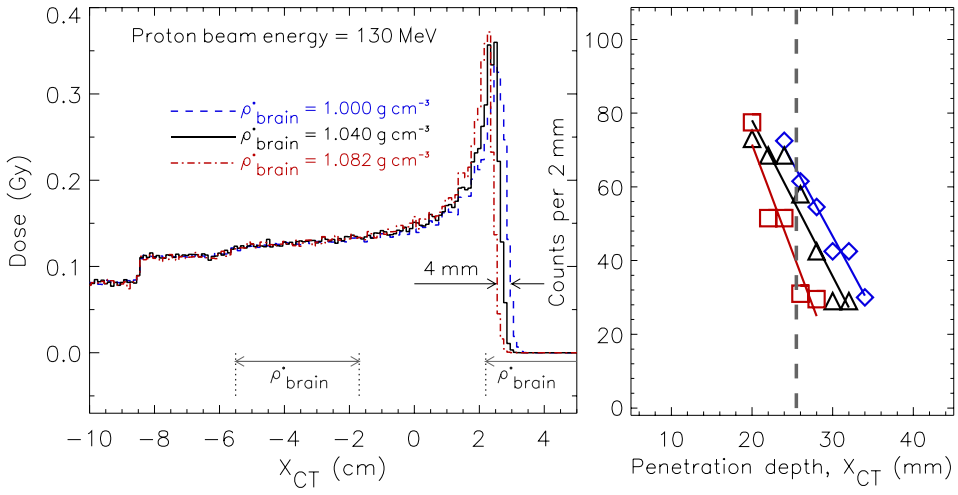

Fig. 25: Left: Depth-dose profiles of proton irradiation in the region of the pituitary gland. Red, black and blue curves correspond to changes in brain density of +4% (scar tissue formation), 0%, and -4% (edema), respectively. The right image shows the peak fall-off region detected with a simulated O-PGI system. A linear regression applied to the different data allows seeing that it is possible to discriminate between the three given scenarios, potentially leading to an automatic trigger when an undesired situation is occurring.

In the short- and mid-term future it is planned to build a multi-pixel, small-scale, multi-slit prompt-gamma camera in order to investigate whether imaging under a therapeutic proton beam condition may reveal benefits in the monitoring of PRT. These efforts comprehend a plethora of developments of instrumentation for medicine (e.g. a data acquisition system that respects the shifting-TOF concept in order to reduce secondary gammas induced by the neutron flux escaping the patient).

Universidad Complutense de Madrid (Spain): (J. Udias et al.)

Contrast enhanced proton range verification via PET emission:

In Madrid there are two facilities for proton therapy under construction, expected to deliver their first proton beams in late 2019-early 2020. They are equipped with IBA and HITACHI accelerators, gantry and delivery rooms. The nuclear physics group (GFN) is establishing collaborations with both facilities in order to put in play all the knowledge in nuclear instrumentation and simulation available at the group. Local funding from the authorities in Madrid has been obtained (http://nuclear.fis.ucm.es/pronto-en) to prepare specific instrumentation for range verification via PET or prompt gamma emissions in these facilities. One of the current research topics targets contrast enhanced proton range verification via PET emission.

When hadrons interact in the patient tissues during hadron therapy sessions, some of the nuclei in the tissue, or even the ions in the therapeutic beam, can experience nuclear transformations, becoming radioactive nuclei. Even if the number of radioactive nuclei produced is very small, they can be detected, located and counted with high precision with nuclear imaging detectors. This makes it possible to verify that the therapeutic dose is being delivered at the prescribed places. Prior to the development of the specific nuclear imaging instrumentation, quantitative estimates of the integral activity produced by protons in biological tissues were generated, specifically addressing the question of an enhancement of this activity production achievable via the use of suitable contrast agents. Those are substances that are administered to the patient to enhance the visibility of the activation due to the deposited dose, in a similar way to the contrast agents that are used in common X-ray or MRI procedures. For instance, Fig. 26 depicts the calculated activities in a tube of 1 cm^2 cross-section after proton irradia-

tion near the Bragg peak in pure water (red line), and in human tissue with a concentration of 5% of a contrast agent based on natural Zn (green line), 120 seconds after the irradiation.

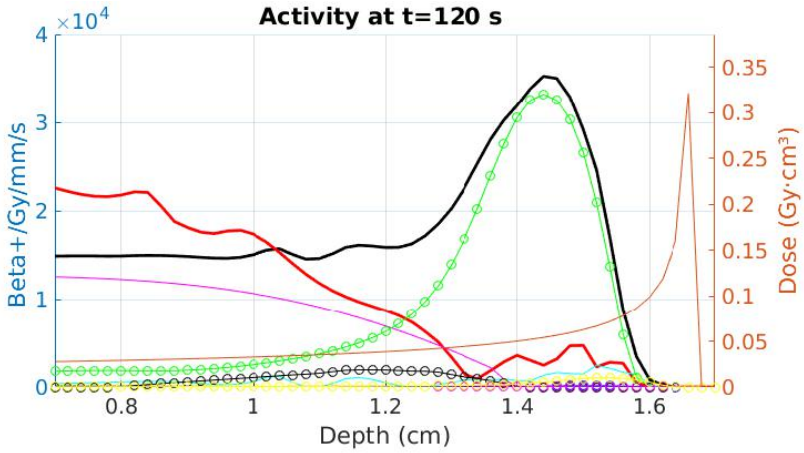

Fig. 26: Calculated activity of different ß$^+$ emitters after irradiation of a tube of 1 cm^2 cross-section with proton beams in pure water (red line) and with a 5% concentration of a contrast agent based on natural Zn (green line), 120 seconds after the irradiation.

Similar values are obtained for the first few seconds after irradiation. Gallium obtained from the nuclear activation of Zn due to hadron therapy beams is visible, and it is also interesting as a nuclear imaging isotope per se, as it shows potential for use in hadron therapy beam range verification [Fraile 2016]. The presence of Zn greatly enhances the activity produced up to 2 mm close to the Bragg peak, which would increase the confidence of range verification. A systematic study of several other potential contrast agents is being performed. Also, identified gaps in the knowledge of relevant cross-sections (needed to perform estimations of the activations of possible contrast agents) are being addressed by proposing the necessary experiments.

Acoustic range verification of proton beams:

Moreover, work was performed on a prototype system for ionoacoustic range verification of proton beams, using low-noise hydrophones and amplifiers and a digital treatment of the acquired signals. When the ions deposit their energy in biological tissue as part of the therapeutical irradiation, part of the energy released appears in the tissue as heat. Consequently, a pressure wave is generated, especially if the hadrons are released in bunches, as it is often the case. This acoustic pressure wave, corresponding to the sound of the hadrons when being stopped in the patient's body, can be recorded with sensitive equipment, and the information gathered can be employed to reconstruct the location and time of the dose deposition, thus allowing for contributing to the verification of the dose delivered. This *ionoacoustic* effect is of current interest [PerezLiva 2017] as an alternative to photon- or charged-particle based range verification techniques.

In the Madrid group the development of prototype hardware has been complemented with detailed simulations of the system (using both Monte Carlo particle transport codes and analytical acoustic wave transport software) and with an analysis of available image reconstruction methods, which can improve the spatial accuracy of the detection system in environments with a low signal-to-noise ratio, as it is the case for proto-acoustic range verification. The system prototype has been tested in local photon LINACs and radiosurgery beams and will soon be irradiated with clinical proton beams. The results of the initial experimental tests and the development of the dose reconstruction algorithms will soon be published [Giza 2018].

The MediNet networking activities have been instrumental to this task. The information exchange with other groups with relevant expertise in range verification (especially, the LMU group in Munich, with ample experience in ionoacoustics) has been fluid and helpful for the progress of our project. At Madrid this has been combined with existing expertise in image reconstruction from ultrasound, in a tomographic fashion. This way experience is gained on how to best use the ultrasound shock wave generated during hadron therapy irradiation for range verification.

Nuclear instrumentation for proton therapy :

Range verification of the hadron therapy procedures is extensively being pursued by measurements of the nuclear radiation produced during irradiation. As in many cases this irradiation is delivered in very short pulses containing a large number of protons. Thus the large instantaneous rates of gamma photons produced, coupled to the, on the other hand, small aggregated number of such photons, represent a challenge for the nuclear instrumentation. The expertise of the Madrid group in designing and operating fast inorganic scintillators is beneficial for the proton range verification with prompt gammas. The fast decay time of $LaBr_3$(Ce) and $CeBr_3$ scintillators (< 20 ns), together with their good efficiency and excellent energy resolution will make it possible to build detectors with high rate capability (in excess of 10 Mcps) and unparalleled spectroscopic capabilities. These constitute extremely interesting devices for proton range verification with prompt gamma emissions. Paving the way towards this goal, tests with one of such detectors were performed [Sanchez 2018] at the Cyberknife^{TM} photon irradiation unit (Accuray Technologies, Sunnyvale CA, USA) at the Hospital Ruber Internacional (Madrid, Spain). The time structure of the photon pulses was perfectly resolved with the detector, as can be seen in the left part of Fig. 27, where the number of pulses against the time measured relative to the trigger signal taken from the electron accelerator is plotted. The photon spectra leaving the head of the Cyberknife irradiation device for an energy setting of 6 MV under different orientations have also been measured (right part of Fig. 27).

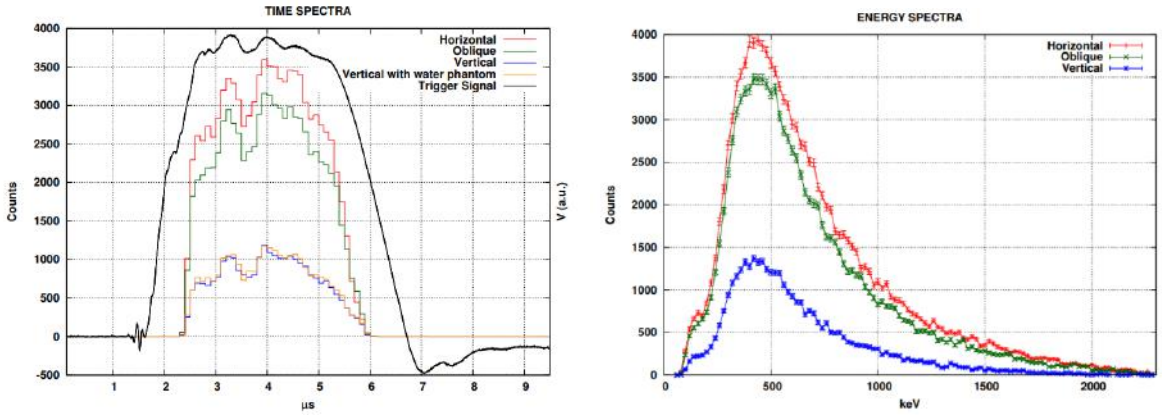

Fig. 27: Left: time structure of photon pulses emitted from a 'Cyberknife' radiotherapy facility (photon energy 6 MeV) measured relative to the trigger pulse derived from the electron accelerator. Right: corresponding photon energy spectra as emitted under different orientations from the beam delivery exit nozzle.

The high rates that such a detector can sustain constitute a demanding challenge for conventional acquisition electronics, if both good energy, timing capabilities and high rates are desired. The conventional electronics commonly employed so far in nuclear experiments will not be sufficient at rates in excess of 2 Mcps. However, current fully digital acquisition systems can handle >1 Gs/s with 12 bits of vertical resolution or better, and by means of PCIe or other fast connections, feed the data to the PC which, with the aid of GPUs and/o multicore computers, can process the data on-the-fly, thus avoiding the huge storage demand required by off-line processing at these rates, without the need for relatively specialized programming skills of embedded FPGA's or

DSP's integrated into the data acquisition boards. The Madrid group has developed specific *in-silico* algorithms to process fully digitized nuclear detector pulses. Fully digitization of the pulses makes them amenable to all kinds of digital algorithms and to deep learning approaches [Sanchez 2018a]. Compared to the conventional DAQ, the fully digital approach performed equally or even better than the conventional one in timing and energy resolution capabilities, while holding the potential to handle much larger rates than the traditional nuclear electronics [Sanchez 2018a]. These achievements will prove particularly useful in proton therapy range verification applications.

KVI-CART, RUG, Groningen, The Netherlands: (P. Dendooven, S. Brandenburg, E. van der Graaf et al.)

In-vivo dose delivery verification using positron emission tomography

As introduced already earlier, a proton or carbon ion beam creates in the patient's body, via nuclear reactions, radioactive nuclides that decay via the emission of positrons. An image of these nuclides can be obtained using positron emission tomography (PET), a well-developed imaging technique used in nuclear medicine for diagnosing disease and evaluating treatment outcome. PET of a radiotherapy irradiation thus gives an image of where the protons or carbon ions have passed and allows, in an indirect way, to verify whether the irradiation was performed according to plan [Parodi 2018] .

The typical use of PET for in-vivo dose delivery verification has a major drawback: information is delayed due to the radioactive half-life (up to 20 minutes) of the positron emitters. The KVI-CART/RUG group in Groningen investigates the possibility of real time feedback by PET of the very short-lived nitrogen-12 nuclide (half-life 11 milliseconds) [Dendooven 2015, Buitenhuis 2017]. Nitrogen-12 imaging puts specific demands on the PET scanner and the detector technology used, both on hardware and software aspects. The scanner needs to image the patient during irradiation and thus a so-called in-situ installation is required. As it should survive for a number of years, it needs to withstand a relatively large radiation dose. The Groningen team showed that novel digital SiPM photosensors are not sufficiently radiation resistant to be used [Diblen 2017] and conclude that any SiPM photosensor considered for an in-situ PET scanner should be checked for sufficient radiation resistance. They are therefore pursuing our research with photomultiplier tube (PMT)-based detectors.

The time structure of the dose delivery in particle therapy depends on the type of accelerator. In order to capture most of the decay of nitrogen-12 nuclides, some special requirements to the PET detectors are needed. If the beam is delivered in time pulses longer than about 10 ms, the PET detector should be capable of measuring good PET signals during the beam pulses. It could be shown that this is possible provided that individual detectors have a small enough surface area so that each can handle its own counting rate, see Fig. 28 [Buitenhuis 2017]. Some accelerators, such as the synchrocyclotron, deliver a very high instantaneous beam intensity. In this case, a PET detector may be blinded during the beam pulses, but should quickly recover, within a few milliseconds, in order not to miss too much of the nitrogen-12 decays. This is an issue for PMT-based detectors.

Real time feedback obviously requires real time data analysis. Standard image reconstructions methods as used in nuclear medicine thus cannot be used. A fast and simple way of obtaining nitrogen-12 profiles from which the range of a proton beam can be determined could be demonstrated. The contribution to the image from longer-lived nuclides can be determined from data taken during the second half of 60-90 millisecond pauses which are introduced into the irradiation and used to obtain a pure nitrogen-12 image. This technique was demonstrated using a small PET system [Buitenhuis 2017].

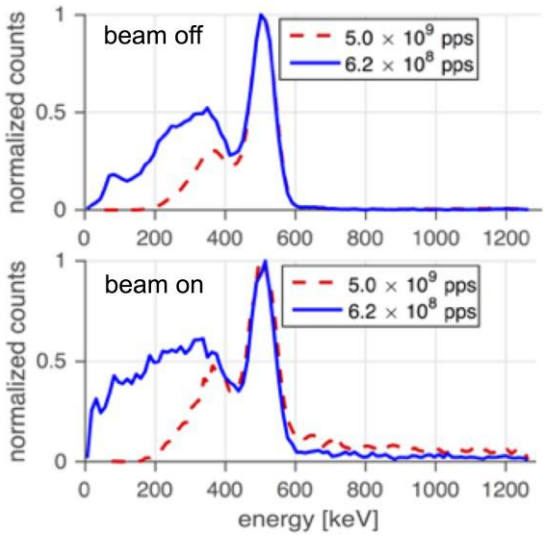

Fig. 28: Gamma-ray energy spectra taken while the proton beam is off (top figure) and on (bottom figure), for 2 values of beam intensities (pps = particles per second). The spectrum quality is identical, showing that suitable PET detectors can take high quality PET data during beam on (Figure adapted from [Buitenhuis 2017]).

Proton radiography:

Currently, proton therapy treatment plans are based on CT-images using one X-ray spectrum (Single Energy CT, SECT). A SECT image quantifies the photon attenuation of a tissue in a CT number which combines information on the tissue's electron density and elemental composition. Using a general correlation between CT number and proton stopping power, the stopping powers for the treatment planning are determined.

The uncertainty in the proton range caused by the uncertainties of the stopping powers deduced from SECT-images amounts, depending on the complexity of the tumour surroundings, up to about 3 %, i.e. 3–6 mm for typical depths of tumours. This uncertainty imposes significant constraints on the treatment planning process (e.g. limitation of possible fields due to critical organs, sub-optimal reduction of dose in healthy tissue). In particular, large uncertainties are associated with situations when the protons pass through materials with significant differences in density or elemental composition. Typical examples of this are the treatment of tumours in the head and neck region, in the lungs and in the lower abdomen. Image reconstruction artefacts for the growing group of patients with prostheses containing ceramic and/or metallic parts complicate the situation even more. In the head and neck region metallic inlays in teeth, present in almost any patient pose serious problems.

In a recently started project the Groningen team studies the potential of advanced X-ray imaging techniques (Dual Energy and spectral CT) *in combination with* proton radiography for stopping power prediction. Protons, in contrast to X-ray photons, are charged particles and lose energy by interacting with electrons and nuclei in matter, leading to multiple Coulomb interactions. Both proton energy loss and scattering can be used for radiographic imaging. Proton imaging has a poorer spatial resolution than X-ray imaging but a higher contrast between different soft tissues. Moreover, proton-based images contain direct information on proton stopping power and do not need a conversion procedure as is the case for photon-based images.

The first aim is to adapt a proton radiography technique that was originally developed at KVI-CART for field flatness assessment and that has recently received renewed interest. In this technique, a scintillation screen is used to image the scattered proton beam by reflecting the scintillation light from a 45° oriented (with respect to the beam direction) mirror towards a CCD camera. As the intensity of the scintillation light is correlated with the proton energy, this technique can also be used to make a proton radiograph of an object that is positioned in the beam line somewhere before the scintillation screen.

Another option for proton radiography that will be studied is to use a kV X-ray flat panel detector at the position of the scintillation screen. In this way, a direct image of the object can be obtained. A recent study showed that these panels can be used for proton imaging with high resolution (0.4 mm pixel pitch) at a dose of approximately 0.1 cGy. There seems to be no real concern regarding radiation hardness issues of the flat panel as no appreciable degradation has been found after an accumulative dose of about 40 Gy.
In using proton radiography in clinical practice for increasing the accuracy of therapy planning, it is obvious that the dose to the patient should be acceptably low, the measurement should only have minor impact on the clinical work flow and, moreover, the accuracy of the information obtained from the radiograph should be such that it can be used to improve/update the CT-based information.
In this project both the scintillation screen-based and the flat panel-based radiography method are investigated and the dose requirements, ease of adoption in the clinic and accuracy of the information are compared.

Perspectives of remaining challenges:
In recent years, the performance of SiPM photosensors for use in scintillation detectors has surpassed that of the standard photomultiplier tubes (PMT). PMTs are known to be very radiation resistant. However, for in-situ PET scanners, sufficiently radiation hard SiPMs need to be developed and tested. Such work is ongoing related to nuclear and particle physics experiments. Improved SiPM photosensors should be tested in a radiotherapy environment.
PET detectors that need to be capable of measuring good PET signals during beam pulses have to operate at very high count rates. This requires the use of dedicated electronics, signal processing and data handling technologies. In case of a radiation rate during beam pulses that cannot possibly be handled by a PET detector, PET detectors need to be developed that can recover within a few milliseconds.

LPC Clermont-Ferrand (France): (G. Montarou et al.)

The activities of the Health Department of LPC Clermont-Ferrand in nuclear instrumentation applied to hadrontherapy are focused on the use of online PET to control the quality of the proton therapy treatment. For this purpose, a small-scale demonstrator has been built (see Fig. 29) and is permanently installed on a beam line at the Antoine Lacassagne clinical proton treatment center in Nice. This allows and will allow for experiments to be conducted regularly with this demonstrator and to study different concepts of quality control. This detector module (DPGA: détecteur pixelisé de grande acceptance, i.e. pixelated detector with large acceptance) is comprised of pixelated BGO scintillator blocks, originating from a recycled Siemens PET scanner and being refurbished for use in the DPGA demonstrator system [Rozes 2016].

Fig. 29: Large-acceptance pixelated detector demonstrator module installed at the 65 MeV proton Medicyc line of the Centre Antoine Lacassage at Nice.

For the next two years, the low energy line (65 MeV proton from the Medicyc proton accelerator) is used outside treatment time to perform these experiments. Subsequently, in 2020, a new room dedicated to research will be available at the CAL in Nice and will provide access to a PBS proton beam of high energy (100-230 MeV).
The instrumental developments planned on this technical platform are:
- Development of a high bandwidth DAQ using the microTCA standard to improve the number of events acquired
- Test of a new reconstruction approach

On the physical aspect, the aim is the possibility of using short-lived radionuclides and in particular ^{12}N to improve the accuracy of the control using this technique, especially in proton therapy with PBS high-energy beams.

The second objective pursued by the Clermont group (in cooperation with a team from Catania/Italy) is to study the potential of improving the biological efficiency of proton therapy using the proton on Boron fusion reaction in the Bragg peak to produce in addition low-range alpha particles at the Bragg peak position.
The rationale behind this alternative treatment modality is the following: while protons at first glance lack distinct radiobiological advantages over photons or electrons, in principle, higher-LET (Linear Energy Transfer) ^{12}C-ions can overcome cancer radio-resistance: DNA lesion complexity increases with LET, resulting in efficient cell killing, i.e. higher Relative Biological Effectiveness (RBE). However, economic and radiobiological issues hamper widespread ^{12}C-ion clinical amenability. Thus, enhancing proton RBE is desirable [Cirrone 2018].
One option could be Boron-Neutron Capture Therapy (BNCT) for the generation of neutron irradiation-triggered alpha particles. BNCT requires thermal neutrons to trigger the reaction where two charged particles (one alpha of 1.77 MeV and one ^{7}Li ion of 1.015 MeV) with a positive Q value of 2.792 MeV are produced [Doi 2008]. The rationale underlying BNCT consists in cancer irradiation by thermal neutrons, which results in a highly localized and mostly lethal targeting of cancer cells because of the very short range and, hence, of the high LET of the low-energy alpha particles generated in the reaction with the ^{10}B atoms. However, despite numerous, carefully designed and generally promising clinical trials [Barth 2012, Kankaanranta 2012], BNCT struggles to establish itself in

clinical routine, both because of the intrinsically challenging quest for ideal carriers to deliver radiobiologically effective concentrations of boron to cancer cells, and because of the limited availability of thermal neutron sources [Barth 2015, Schwint 2015].

The alternative proton boron capture therapy (PBCT) method was recently demonstrated experimentally for the first time in [Cirrone2018] to enhance proton therapy effectiveness. According to the description given in [Cirrone 2018], the p + ^{11}B → 3α nuclear fusion reaction at low energy (theoretically proposed before in simulation studies [Barth 2012]) can be understood as a two-step reaction due to its behavior at the three resonant energies (0.162 MeV, 0.675 MeV and 2.64 MeV). Firstly, a proton, interacting with ^{11}B, induces the formation of a ^{12}C* compound nucleus formed in the 2- or 3$^-$ excited state. If the ^{12}C* nucleus is formed in its 2$^-$ state, it will decay to the first 2$^+$ state of ^{8}Be emitting one alpha particle. If the ^{12}C* nucleus is formed in its 3$^-$ state, then the primary alpha particle can be emitted either from the decay to the first 2$^+$ state ^{8}Be state, or from the decay to the 0$^+$ ^{8}Be ground state. In either case, the remaining ^{8}Be nucleus immediately decays into two secondary alpha particles. For low proton energies (0.1 – 5 MeV) the reaction cross section becomes significantly high (with a maximum of 1.2 barn [Kankaanranta 2012]), thus maximizing the (short-range, high-LET) alpha particle production around the Bragg peak region, which is advantageous for an alternative proton therapy approach. The three alpha particles are effective in inducing the death of a tumor cell. After boron is accumulated in the tumor region, the incident therapeutic proton beam can react with the boron in the tumor region. An increase of the proton's maximum dose level is caused by the boron and only the tumor cell is damaged more critically [Barth 2012].

CONCLUDING REMARKS

Medical imaging, both for applications in diagnostics and treatment in nuclear medicine and hadron tumor therapy, for which the detection of radiation emitted by the atomic nucleus is involved, has experienced and continues to exhibit evolution at exponential speeds. In the past, this evolution has largely benefited from technologies developed and tested in the experimental nuclear physics area, and it seems that this trend will only increase in the future. The maturity of the nuclear imaging sector can be seen by the fact that while in the past most nuclear detection instrumentation technologies employed in the medical field, such as photomultiplier tubes and scintillation crystals, were borrowed from the experimental nuclear physics knowledge base, nowadays new technologies are being pursued by the demanding medical industry, where the rate of technological evolution has never been so fast and new techniques are translated into biomedical research and clinical use within short periods.

Nuclear physics research groups have always been aware that their work in radiation detection, simulations, signal processing and data acquisition electronics, as well as data processing, might find applications in the medical field. But today it can be realized that the ongoing activities in these two fields are not only complementary and synergetic, but that their pace of development is very different. Nuclear physics experiments may take several years to be designed, funded, set up, run and analyzed. In the medical imaging arena, though, trends and technologies are being introduced, tested and dismissed at high speed. One can assess this by attending every year the leading conferences in the (nuclear) medical imaging instrumentation sector, such as the IEEE Medical Imaging Conference, witnessing how the trends of the previous year have been discarded and new ones are moving into the focus [NuPECC 2014].

The present document could only give a snapshot glimpse into the wide range of activities on cutting-edge research efforts in the realm of nuclear instrumentation for the medical field, in particular for various modalities of medical imaging, responding to pressing societal needs. Nevertheless, it is the goal of this text to convey the message that the European landscape of applied research in the area of medical physics, routed in nuclear instrumentation developments and aiming at translating nuclear concepts into practical applicability in the medical field, is well prepared to meet the upcoming challenges.

Along the specific R&D work pursued in each research institution goes an interdisciplinary cooperation between medical doctors and medical physicists in clinical practice, assisted by professional networks like the Particle Therapy Cooperation Group (PTCOG) in the worldwide growing field of hadron therapy, national and international professional societies of Medical Physicists or, last but not least, also networking activities like the MediNet activity within the European ENSAR2 Integrating Initiative, bringing together research physicists and medical physics practitioners at clinical centers.

REFERENCES AND APPLICABLE DOCUMENTS

[Abellan 2013] C. Abellan, J.-P. Cachemiche, F. Réthoré, and C. Morel , *A data acquisition system for medical imaging*, In: 2013 3rd International Conference on Advancements in Nuclear Instrumentation, Measurement Methods and their Applications (ANIMMA), pp. 1–7 (2013), DOI: 10.1109/ANIMMA.2013.6728028

[Aldawood 2015] Aldawood, S., Castelhano, I., Gernhäuser, R., v.d. Kolff, H., Lang, C., Lutter, R., Maier, L., Marinsek, T., Schaart, D.R., Parodi, K., Thirolf, P.G., *Comparative characterization study of a $LaBr_3$(Ce) scintillation crystal in two surface wrapping scenarios: absorptive and reflective,* Frontiers in Oncology 5, 270 (2015).

[Aldawood 2017] Aldawood, S, Thirolf, P.G., Miani, A., Böhmer, M., Dedes, G., Gernhäuser, R., Lang, C., Liprandi, S., Maier, L., Marinsek, T., Mayerhofer, M., Schaart, D.R., Valencia Lozano, I., Parodi, K., *Development of a Compton Camera for prompt-Gamma Medical Imaging,* Radiation Physics and Chemistry 140C, 190-197 (2017).

[Assmann 2015] W. Assmann, S. Kellnberger S, S. Reinhardt, S. Lehrack, A. Edlich, P.G. Thirolf, M. Moser, G. Dollinger, M. Omar, V. Ntziachristos, K. Parodi, *Ionoacoustic characterization of the proton Bragg peak with submillimeter accuracy*, Med. Phys. 42 567–74 (2015).

[Barrio 2017] J. Barrio, A. Etxebeste, L. Granado, E. Muñoz, J.F. Oliver, A. Ros, J. Roser, C. Solaz and G. Llosá, *Performance improvement tests of MACACO: a Compton telescope based on continuous crystals and SiPMs,* Nucl. Instr. Meth. A 912, 48-52 (2018), https://doi.org/10.1016/j.nima.2017.10.033.

[Barth 2012] R.F. Barth, M. H. Vicente, O.K. Harling, W.S. Kiger, K. J. Riley, P. J. Binns, F. M. Wagner, M. Suzuki, T. Aihara, I. Kato, S. Kawabata, *Current status of Boron neutron capture therapy for high grade gliomas and recurrent head and neck cancer*, Radiation Oncology **7**, 146 (2012), https://doi.org/10.1186/1748-717X-7-146.

[Barth 2015] R.F. Barth, *From the laboratory to the clinic: How translational studies in animals have led to clinical advances in boron neutron capture therapy*, Appl. Radiat. Isot. **106**, 22–28 (2015).

[Biegun 2012] A.K. Biegun, E. Seravalli, P. Cambraia Lopes, I. Rinaldi, M. Pinto, D.C. Oxley, P. Dendooven, F. Verhaegen, K. Parodi, P. Crespo, D.R. Schaart, *Time-of-flight neutron rejection to improve prompt gamma imaging for proton range verification: a simulation study*, Phys. Med. Biol. 57, 6429 – 6444 (2012). (http://dx.doi.org/10.1088/0031-9155/57/20/6429).

[Bisogni 2017] M.-G.. Bisogni et al., *INSIDE in-beam positron emission tomography system for particle range monitoring in hadron therapy*, Journal of Medical Imaging 4-011005-1-12 (2017).

[Borras 2016] Borras J.M., Lievens Y., Barton M, Corral J, Ferlay J, Bray F, Grau C, *How many new cancer patients in Europe will require radiotherapy by 2025?*, An ESTRO-HERO analysis , Radiotherapy and Oncology 119, 5-11 (2016).

[Buitenhuis 2017] H.J.T. Buitenhuis, F. Diblen, K.W. Brzezinski, S. Brandenburg, P. Dendooven, *Beam-on imaging of short-lived positron emitters during proton therapy,* Phys. Med. Biol. 62 , 4654 (2017).

[CambraiaLopes 2018] P. Cambraia Lopes, P. Crespo, H. Simões, R. Ferreira Marques, K. Parodi, D.R. Schaart, *Simulation of proton range monitoring in an anthropomorphic phantom using multi-slat collimators and time-of-flight detection of prompt-gamma quanta,* Physica Medica 54, 1-14 (2018). (https://doi.org/10.1016/j.ejmp.2018.09.001)

[CambraiaLopes 2015] P. Cambraia Lopes, E. Clementel, P. Crespo, S. Henrotin, J. Huizenga, G. Janssens, K. Parodi, D. Prieels, F. Roellinghoff, J. Smeets, F. Stichelbaut, D.R. Schaart, T*ime-resolved imaging of prompt-*

gamma rays for proton range verification using a knife-edge slit camera based on digital photon counters, Phys. Med. Biol. 60, 6063-6085 (2015) (http://dx.doi.org/10.1088/0031-9155/60/15/6063)

[CambraiaLopes 2017] P. Cambraia Lopes, *Time-resolved imaging of secondary gamma ray emissions for in vivo monitoring of proton therapy: Methodological and experimental feasibility studies*, PhD thesis, TU- Delft, The Netherlands, 2017 (https://doi.org/10.4233/uuid:3ba81eb3-3278-411b-abc2-effdbb119991)

[CambraiaLopes 2011] P. Cambraia Lopes, P. Crespo, J. Huizenga, D.R. Schaart, *Optimization of the signal-to-background ratio in prompt gamma imaging using energy- and shifting time-of-flight discrimination: experiments with a scanning parallel-slit collimator*, IEEE Trans. Radiat. Plasma Med. Sci. 2, 510-519 (2011), (http://dx.doi.org/10.1109/TRPMS.2018.2846612)

[Ciciriello 2013] F. Ciciriello *et al.*, *BASIC32_ADC, a front-end ASIC for SiPM detectors,* in *Proc. IEEE NSS/MIC*, Oct./Nov. 2013, pp. 1–6.

[Cirrone 2018] G.A.P. Cirrone et al., *First experimental proof of proton boron capture therapy (PBCT) to enhance proton therapy effectiveness*, Scientific Reports **8**, 1141 (2018).

[Collot 2017] J. Collot, A. Bes, G. Bosson, S. Curtoni, D. Dauvergne, L. Gallin-Martel, M.-L. Gallin-Martel, J.-F. Muraz, J. Hostachy, A. Lacoste, S. Marcatili, F. Rarbi, M. Yamouni, J.-M. Brom, J. Morse, W. De Nolf, M. Salomé, J. Krimmer, É. Testa, The European Physical Society Conference on High Energy Physics, 5-12 July, 2017, Venice. PoS(EPS-HEP2017)781. https://pos.sissa.it/314

[Dauvergne 2016] Dauvergne D., Krimmer K., Testa E., *A method of detecting a difference between a characteristic foretold and an actual characteristic of a hadron beam*; 2016-07-94, App/Pub number FR1656378A.

[Dendooven 2015] P. Dendooven et al, S*hort-lived positron emitters in beam-on PET imaging during proton therapy,* Phys. Med. Biol. 60 (2015) 8923.

[Denham 2002] J. Denham and M. Hauer-Jensen, T*he radiotherapeutic injury — a complex wound*, Radiother. Oncol. 63, 129–145 (2002).

[Diblen 2017] F. Diblen et al., *Radiation Hardness of dSiPM Sensors in a Proton Therapy Radiation Environmen*t, IEEE Trans. Nucl. Sci. 64 (2017) 7.

[Doi 2008] Doi, A., Kawabata, S., Lida, K., Yokoyama, K. & Kajimoto, Y. et al., T*umour-specific targeting of sodium borocaptate (BSH) to malignant glioma by transferrin-PEG liposomes: a modality for boron capture therapy*, Neurooncol. **87**, 287-294 (2008).

[Everett 1977] D. Everett, J. Fleming, R. Todd, J. Nightingale, *Gamma-radiation imaging system based on the Compton effect*, Proc. Inst. Electr. Eng. 124, 995 (1977). doi:doi:10.1049/piee.1977.0203

[Fabbro 2017] R. Fabbro, PhD thesis, Univ. Grenoble-Alpes, 2017: https://primes.universite-lyon.fr/labex-primes/version-francaise/navigation/recherche/wp-1-methodes-et-instrumentations-innovantes-en-radiotherapies/robin-fabbro-2014-2017-phd-director-yannick-arnoud-co-director-jean-francois-adam-15854.kjsp?RH=1533115571711

[Ferrero 2018] Ferrero V, Fiorina E, Morrocchi M, Pennazio F, et al., *Online proton therapy monitoring: clinical test of a silicon-photodetector-based in-beam PET.* Scientific Reports 8, 4100 (2018).

[Fiorina 2018] Fiorina E, Ferrero V, Pennazio F, et al., *Monte Carlo simulation tool for online treatment monitoring in hadrontherapy with in-beam PET: A patient study*, Physica Medica EJMP 2018; in press, https://doi.org/10.1016/j.ejmp.2018.05.002.

[Fontana 2018] Fontana M., Dauvergne D., Della Negra R., Létang J. M., Mounier F., Testa É., Zanetti L., Zoccarato Y. L*arge surface gamma cameras for medical imaging: characterization of the bismuth germanate blocks,* Journal of Instrumentation 13 P08018. (2018).

[Fontana 2017] Fontana M., Dauvergne D., Létang J. M., Ley J.-L., Maxim, V., Testa É. Versatile Compton camera for high energy gamma rays: Monte Carlo comparison with Anger camera for medical imaging, Acta Physica Polonica B 48, 1639-1645 (2017). DOI: 10.5506/AphysPolB.48.1639.

[Fontana 2017a] Fontana M., Dauvergne D., Létang J. M., Ley J.-L., Testa É., *Compton camera study for high efficiency SPECT and benchmark with Anger system*, Phys. Med. Biol. 62, 8794-8812 (2017).

[Fraile 2016] Fraile LM, Herraiz JL, Udías JM, Cal-González J, Corzo PMG, España S, herranz E, Pérez-Liva M, Picado E, Vicente E, Muñoz-Martín A, Vaquero JJ, *Experimental validation of gallium production and isotope-dependent positron range correction in PET,* Nucl. Instr. Meth. A 814, 110-116 (2017), DOI:10.1016/j.nima.2016.01.013

[GallinMartel 2016] L. Gallin-Martel, O. Rossetto, Y. Arnoud, B. Boyer, R. Delorme, R. Fabbro, ML. Gallin-Martel, O. Guillaudin, A. Pélissier, 2016 IEEE Nuclear Science Symposium, Medical Imaging Conference and Room-Temperature Semiconductor Detector Workshop (NSS/MIC/RTSD), pp.1-5, 2016, http://2016.nss-mic.org/index.php , doi：10.1109/NSSMIC.2016.8069397

[GallinMartel 2018] M.-L. Gallin-Martel, L. Abbassi, A. Bes, G. Bosson, J. Collot, T. Crozes, S. Curtoni, D. Dauvergne, W. De Nolf, M. Fontana, L. Gallin-Martel, J.-Y. Hostachy, J. Krimmer, A. Lacoste, S. Marcatili, J. Morse, J.-F. Motte, J.-F. Muraz, F. E. Rarbi, O. Rossetto, M. Salomé, É. Testa, R. Vuiart and M. Yamouni, Proceedings of ANIMMA 2017, Liège, Belgium, June 19-23, 2017, EPJ Web of Conferences 170 (2018) 09005, https://doi.org/10.1051/epjconf/201817009005

[Giza 2018] Giza, Olivia; Sanchez-Parcerisa, Daniel; Sanchez-Tembleque, Victor; Herraiz, Joaquin; Camacho, Jorge; Avery, Stephen; Udías, José Manuel. *Photoacoustic dose monitoring in clinical high-energy photon beams.* Phys. Med. Biol. (submitted, 2018).

[Golnik 2014] C. Golnik, F. Hueso- González, A. Müller, P. Dendooven, W. Enghardt, F. Fiedler, T. Kormoll, K. Roemer, J. Petzoldt, A. Wagner, G. Pausch, *Range assessment in particle therapy based on prompt γ-ray timing measurements*, Phys. Med. Biol. 59 (2014) 5399-5422. http://dx.doi.org/10.1088/0031-9155/59/18/5399

[Hueso-Gonzalez 2015] F. Hueso-González, W. Enghardt, F. Fiedler, C. Golnik, G. Janssens, J. Petzoldt, D. Prieels, M. Priegnitz, K. E. Römer, J. Smeets, F. V. Stappen, A. Wagner, G. Pausch, *First test of the prompt gamma ray timing method with heterogeneous targets at a clinical proton therapy facility,* Phys. Med. Biol. 60 (16) (2015) 6247. doi:10.1088/0031-9155/60/16/6247.

[Kankaanranta 2012] L. Kankaanranta,T. Seppala, H. Koivunoro, K. Saarilahti et al, *Boron neutron capture therapy in the treatment of locally recurred head-and-neck cancer: final analysis of a phase I/II trial*, Int. Jour. of Rad. Onc. Biol. Phys. **82**, e67-e75 (2012).

[Kögler 2018] T. J. Kögler, J. Berthold, B. Deneva, W. Enghardt, K. E. Roemer, A. Straessner, A. Wagner, T. Werner, G. Pausch, *Proving the Concept of Single Plane Compton Imaging for Radionuclide and Prompt Gamma-Ray*

Imaging, Paper JS-03 presented at the 2018 IEEE Nuclear Science Symposium and Medical Imaging Conference, Sydney, Australia, Nov. 10-17, 2018.

[Krimmer 2015] Krimmer, J., Ley, J.-L., Abellan, C., Cachemiche, J.-P., Caponetto, L., Chen, X., Zoccarato, Y. (2015). *Development of a Compton camera for medical applications based on silicon strip and scintillation detector*s, Nucl. Instr. Meth. A 787, 98–101 (2015).

[Krimmer 2017] J. Krimmer, G. Angellier, L. Balleyguier, D. Dauvergne, N. Freud, J. Hérault, J. Létang, H. Mathez, M. Pinto, E. Testa, Y. Zoccarato, *A cost-effective monitoring technique in particle therapy via uncollimated prompt gamma peak integration,* Applied Physics Letters 110 (2017) 154102. doi:10.1063/1.4980103.

[Krimmer 2018] J. Krimmer, D. Dauvergne, J.M. Létang, É. Testa, *Prompt-gamma monitoring in hadrontherapy: A review,* Nucl. Instr. Meth. A 878, 58-73 (2018), http://dx.doi.org/10.1016/j.nima.2017.07.063

[Lang 2012] Lang, C. , Habs, D. Thirolf, P.G. Zoglauer, A., *Submillimeter nuclear medical imaging with a Compton Camera using triple coincidences of collinear β^+-annihilation photons and γ rays*, Radiotherapy and Oncology 102, s1 (2012), S29.

[Lang 2014] Lang, C., Habs, D., Parodi, K., Thirolf, P.G., S*ubmillimeter nuclear medical imaging with increased sensitivity in positron emission tomography using β^+-γ coincidence*s, Jour. of Instrumentation 9 (2014) P01008.

[Lehrack 2017] S. Lehrack, W. Assmann D. Bertrand, S. Henrotin, J. Herault, V. Heymans, P.V. Stappen, P.G. Thirolf, M. Vidal, J. Van de Walle, K. Parodi, *Submillimeter ionoacoustic range determination for protons in water at a clinical synchrocyclotron*, Phys. Med. Biol. 62 L20 (2017).

[Liprandi 2017] Liprandi, S., Mayerhofer, M., Aldawood, S., Binder, T., Dedes, G., Miani, A., Schaart, D.R., Valencia Lozano, I., Parodi, K., Thirolf, P.G., S*ub-3mm spatial resolution from a large monolithic $LaBr_3$(Ce) scintillator*, Current Directions in Biomedical Engineering 3 (2017) 655-659.

[Marafini 2015] Marafini M, Attili A, Battistoni G, Belcar N., Bisogni MG, Camarlinghi N et al., T*he INSIDE Project: Innovative Solutions for In-Beam Dosimetry in Hadrontherapy*. Acta Physica Polonica A127 (2015) 1465.

[Marafini 2017] M. Marafini *et al.*, MONDO: *A neutron tracker for particle therapy secondary emission characterisation*, Phys. Med. Biol. 62, 3299–3312 (2017), doi: 10.1088/1361-6560/aa623a.

[Martins 2017] P. Magalhaes Martins, R. Dal Bello, A. Rinscheid, K. Roemer, T. Werner, W. Enghardt, G. Pausch, J. Seco, Current Directions in Biomedical Engineering 2017; 3(2): 113–117.

[Moteabbed 2011] M. Moteabbed, S. España, H. Paganetti, *Monte Carlo patient study on the comparison of prompt gamma and PET imaging for range verification in proton therapy,* Phys. Med. Biol. 56, 1063-1082 (2011).

[Munoz 2017] Muñoz, E., Barrio, J., Etxebeste, A., Garcia Ortega, P., Lacasta, C., Oliver, J., Solaz, C., and Llosá, G., *Performance evaluation of MACACO: a multilayer Compton camera,* Phys. Med. Biol. 62 7321 -7341(2017). https://doi.org/10.1088/1361-6560/aa8070.

[Munoz 2018] E. Muñoz, J. Barrio, D. Bemmerer, A. Etxebeste, F. Fiedler, F. Hueso-González, C. Lacasta, J. F. Oliver, K. Römer, C. Solaz, L. Wagner and G. Llosá, *Tests of MACACO Compton telescope with 4.44 MeV gamma rays,* JINST 13 P05007 (2018).

[Munoz 2018a] E. Muñoz, J. Barrio, J. Bernabéu, A. Etxebeste, C. Lacasta, G. Llosá, A. Ros, J. Roser and J. F. Oliver, *Noise evaluation of Compton camera imaging for proton therapy*, Phys. Med. Biol. 63 (2018) 13.

[Muraro 2006] S. Muraro et al, *Monitoring of Hadron therapy Treatments by Means of Charged Particle Detection,* Front. Oncol. 6, 177 (2016).

[Newhauser 2011] W. D. Newhauser and M. Durante, A*ssessing the risk of second malignancies after modern radiotherapy*, *Nature Rev. Cancer* 11, 438–448 (2011).

[NuPECC 2014] *Nuclear Physics for Medicine*, edited by: F. Azaiez, A. Bracco, J. Dobeš, A. Jokinen, G.-E. Körner, A. Maj, A.Murphy and P. Van Duppen, NuPECC (2014). ISBN: 978-2-36873-008-9.

[Ortega 2015] P.G. Ortega, I. Torres-Espallardo, F. Cerutti, A. Ferrari, J. E. Gillam, C. Lacasta, G. Llosá, J. F. Oliver, P.R. Sala, P. Solevi and M. Rafecas, *Study and comparison of different sensitivity models for a Compton Telescope,* Phys. Med. Biol. 60, 1845 -1863 (2015).

[Parodi 2015] K. Parodi and W. Assmann, *Ionoacoustics: A new direct method for range verification,* Mod. Phys. Lett. A 30 1540025 (2015).

[Parodi 2016] K. Parodi, *On- and off-line monitoring of ion beam treatment*, Nucl. Instr. Meth. A 809, 113-119, (2016); doi:10.1016/j.nima.2015.06.056.

[Parodi 2018] K. Parodi and J.C. Polf, *In vivo range verification in particle therapy*, Med. Phys. 45 (2018) e1036.

[Pausch 2016] G. Pausch, J. Petzoldt, M. Berthel, W. Enghardt, F. Fiedler, C. Golnik, F. Hueso-González, R. Lentering, K. Römer, K. Ruhnau, J. Stein, A. Wolf, T. Kormoll, *Scintillator-Based High-Throughput Fast Timing Spectroscopy for Real-Time Range Verification in Particle Therapy,* IEEE Trans. Nucl. Sci. 63 (2016) 664-672. http://dx.doi.org/10.1109/TNS.2016.2527822

[Pausch 2018] G. Pausch, J. Berthold, W. Enghardt, K. Römer, A. Straessner, A. Wagner, T. Werner, T. Kögler: D*etection systems for range monitoring in proton therapy: Needs and challenges,*
Nucl. Instr. Meth. A (2018), in print. https://doi.org/10.1016/j.nima.2018.09.062

[Pausch 2018a] G. Pausch, C. Mueller, J. Berthold, W. Enghardt, K. Römer, J. Stein, A. Straessner, A. Wagner, T. Werner, A. Wolf, and T. Kögler, *Effect of Strong Load Variations on Gain and Timing of $CeBr_3$ Scintillation Detectors Used for Range Monitoring in Proton Radiotherapy,* Paper M-03-421 presented at the 2018 IEEE Nuclear Science Symposium and Medical Imaging Conference, Sydney, Australia, Nov. 10-17, 2018.

[Pausch 2016] G. Pausch, C. Golnik, A. Schulz, W. Enghardt, *A Novel Scheme of Compton Imaging for Nuclear Medicine*, Paper N60-1 presented at the 2016 IEEE Nuclear Science Symposium in Strasbourg, France, Oct. 29 – Nov. 6, 2016; 2016 IEEE NSS/MIC Conference Record. https://doi.org/10.1109/NSSMIC.2016.8069921

[PerezLiva 2017] Pérez-Liva M, Herraiz JL, Udias JM, *Time domain reconstruction of sound speed and attenuation in ultrasound computed tomography using full wave inversion,* J. Acoust. Soc. Am. 141, 1595- 1604 (2017),**DOI:** dx.doi.org/10.1121/1.4976688.

[Piersanti 2014] L. Piersanti *et al.*, *Measurement of charged particle yields from PMMA irradiated by a 220 MeV/u $^{(12)}C$ beam,* Phys. Med. Biol. 59, 1857 (2014).

[Rozes 2016] A. Rozes, C*onstruction et premières caractérisations d'un détecteur dédié à la mesure de l'activité β^+ induite lors des traitements d'hadronthérapie, en vue de leur contrôle balistique*. Autre [cond-mat.other]. Université Blaise Pascal - Clermont-Ferrand II (2016), https://tel.archives-ouvertes.fr/tel-01477171.

[Sanchez 2018] V. Sánchez-Tembleque, D. Sánchez-Parcerisa, V. Valladolid-Onecha, L.M. Fraile, J.M. Udías, *Simultaneous measurement of the spectral and temporal properties of a LINAC pulse from outside the treatment room,* Rad. Phys. Chem. (submitted, 2018).

[Sanchez 2018a] V. Sánchez-Tembleque, V. Vedia, L. M. Fraile, S. Ritt, J. M. Udías, *Optimizing Time-Pickup Algorithms in Radiation Detectors with a Genetic Algorithm,* Nucl. Instr. Meth. Phys A. (submitted, 2018)

[Schaart 2010] D.R. Schaart, S. Seifert, R. Vinke, H.T. van Dam, P. Dendooven, H. Löhner, F.J. Beekman, *LaBr 3 :Ce and SiPMs for time-of-flight PET: achieving100 ps coincidence resolving time,* Phys. Med. Biol. 55, N179 - N189, 2010.

[Schwint 2015] A.E. Schwint & V.A. Trivillin, '*Close-to-ideal' tumor boron targeting for boron neutron capture therapy is possible with 'less-than-ideal' boron carriers approved for use in humans*, Ther. Deliv. **6**, 269-272 (2015).

[Solevi 2018] P. Solevi, E. Muñoz, C. Solaz, M. Trovato, P. Dendooven, J. Gillam, C. Lacasta, J. Oliver, M. Rafecas, I. Torres-Espallardo, G. Llosá, Gabriela, *Performance of MACACO Compton Telescope for Ion-Beam Therapy Monitoring: first test with proton beams*, Phys. Med. Biol. 61, 5149-5165 (2016).

[Spraker 2012] M.C. Spraker et al., T*he $^{11}B(p,\alpha)^{8}Be \rightarrow \alpha + \alpha$ and the $^{11}B(\alpha,\alpha)^{11}B$ reactions at energies below 5.4 MeV,* Jour. Fusion Energy **31**, 357-367 (2012).

[Thirolf 2013] Thirolf, P., Aldawood, S., Lang, C., Parodi, K., *Development of a Compton Camera for Online Range Monitoring of Laser-Accelerated Proton Beams,* Med. Phys. 40, 144 (2013).

[Thirolf 2014] Thirolf, P.G., Lang, C., Aldawood, S., v.d. Kolff, H.G., Maier, L., Schaart, D.R., Parodi, K., *Development of a Compton Camera for Online Range Monitoring of Laser-Accelerated Proton Beams via Prompt-Gamma Detection,* EPJ Web of Conferences 66, 11036 (2014).

[Thirolf 2015] Thirolf, P.G., Lang, C. and Parodi, K., *Perspectives for highly-sensitive PET-based medical imaging using β^{+} γ coincidences*, Acta Physica Polonica A 127, 1441 (2015).

[Thirolf 2016] Thirolf, P.G., Aldawood, S., Böhmer, M., Bortfeldt, J., Castelhano, I., Dedes, G., Fiedler, F., Gernhäuser, R. Golnik, C., Helmbrecht, S., Hueso-Gonzalez, F., v.d. Kolff, H., Kormoll, T., Lang, C., Liprandi, S., Lutter, R., Marinsek, T., Maier, L., Pausch, G., Petzoldt, J., Römer, K., Schaart, D., Parodi, K., *Development of a Compton Camera Prototype for Medical Imaging*, EPJ Web of Conferences 117, 05005 (2016).

[Traini 2017] G. Traini et al., D*esign of a new tracking device for on-line beam range monitor in carbon therapy,* Physica Medica 34 (2017) 18-27.

[Verburg 2014] Verburg JM, Seco J, *Prompt range verification through prompt gamma-ray spectroscopy,* Phys. Med. Biol. 59, 7089-7106 (2014).

[Verburg 2014a] J.M. Verburg, Reducing Range Uncertainty in Proton Therapy, PhD thesis, Eindhoven University of Technology, The Netherlands (2014); ISBN 978-90-386-3849-2.

[Werner 2017] T. Werner, J. Berthold, W. Enghardt, F. Hueso González, T. Kögler, J. Petzoldt, C. Richter, A. Rinscheid, K. Römer, K. Ruhnau, J. Smeets, J. Stein, A. Straessner, A. Wolf, and G. Pausch, *Range Verification in Proton Therapy by Prompt Gamma-Ray Timing (PGT): Steps towards Clinical Implementation,* Paper M-11-04 presented at the 2017 IEEE Nuclear Science Symposium and Medical Imaging Conference, Atlanta, USA, Oct. 23-28, 2017.

[Werner 2018] T. Werner, J. Berthold, F. Hueso-Gonzalez, T. Koegler, J. Petzoldt, K. Roemer, C. Richter, A. Rinscheid, A. Straessner, W. Enghardt, and G. Pausch, *Processing of prompt gamma-ray timing data for proton range measurements at a clinical beam delivery,* Paper submitted to Phys. Med. Biol. (2018), under review.

[Yoon 2014] D.-K. Yoon, J.-Y Sung and T.S. Suh, *Application of proton boron fusion reaction to radiation therapy: a Monte-Carlo simulation study,* Appl. Phys. Lett. **105**, 223507 (2014).